Virtual International Seminar on Theoretical Advancements

2022.3.30

Model Construction and TD-DMRG Simulation for Exciton Dynamics in Molecular Aggregated Systems

Haibo Ma

School of Chemistry and Chemical Engineering,
Nanjing University, Nanjing 210023, China

https://itcc.nju.edu.cn/haibo/

haibo@nju.edu.cn

Outline

- **Background: Exciton dynamics**

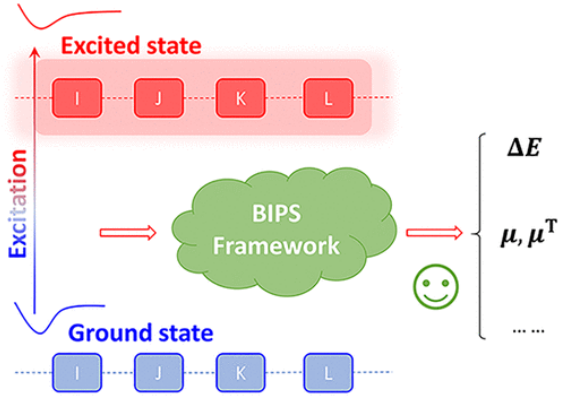

- **Model construction**
  - **Automatic construction of excitonic basis**
  - **Evaluation of exciton-phonon couplings**

- **Quantum dynamics simulation**
  - **Time-dependent density matrix renormalization group (TD-DMRG)**
  - **Stochastic adaptive single-site TD-DMRG**

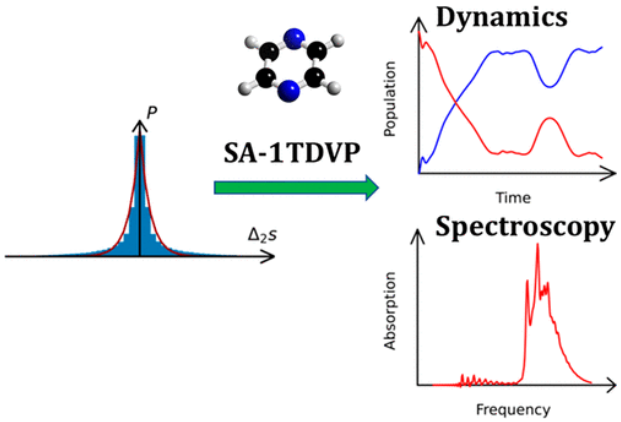

Excited States in Large Photoactive Systems

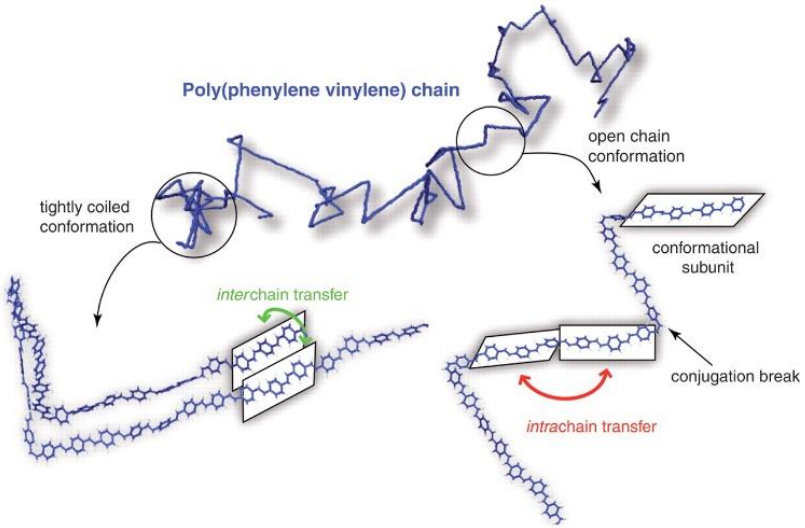

Intrachain Energy Transfer in a Conjugated Polymer

E. Collini, G. D. Scholes, *Science* **2009**, 323, 369

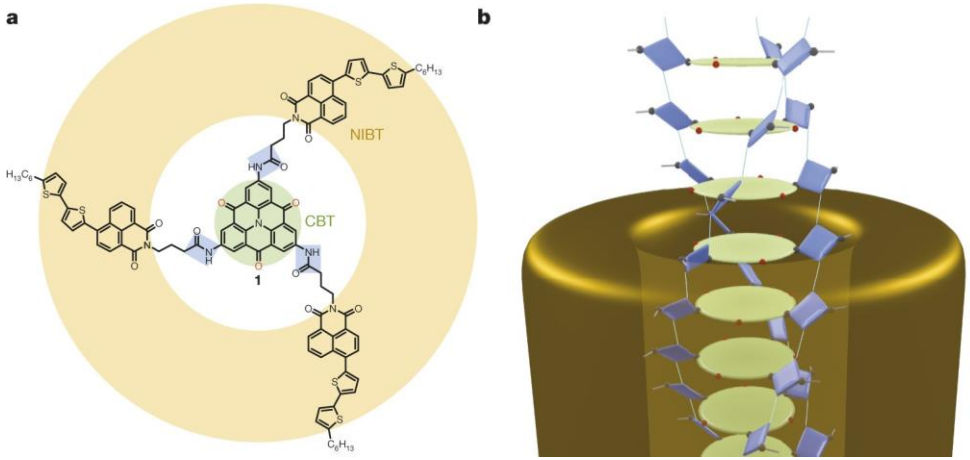

Long-range energy transport in single supramolecular nanofibres

A. T. Haedler, et al., *Nature* **2015**, 523, 196

Both the electronic structure and quantum dynamics of large photoactive systems can hardly be simulated by standard quantum chemistry methods.

Excitonic Model Hamiltonians

Exciton: a bound electron-hole pair → a quasi-particle

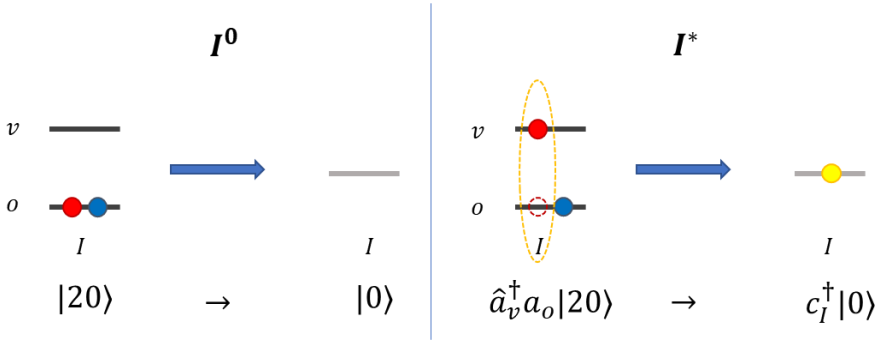

Real system

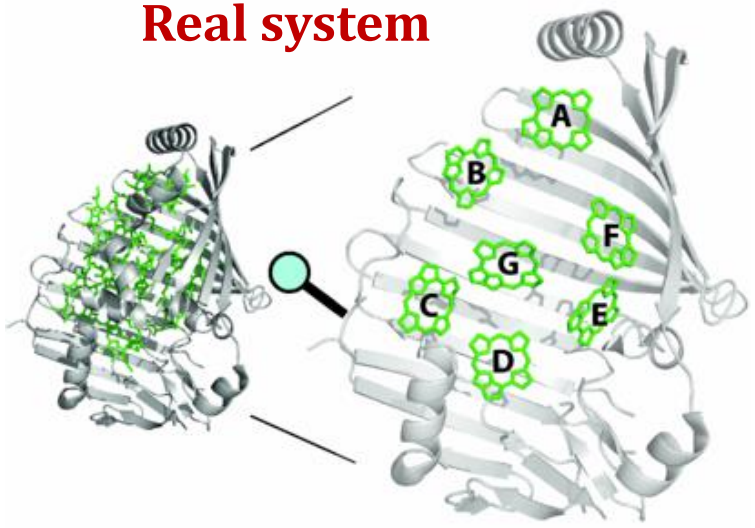

Fenna–Matthews–Olson (FMO) bacteriochlorophyll complex

Simplification

Excitonic model

$$\hat{H}_{\text{ex}} = \sum_{i=1}^{7} \varepsilon_i \hat{c}_i^\dagger \hat{c}_i + \sum_{i \neq j} V_{ij} \hat{c}_i^\dagger \hat{c}_j$$

(7×7) matrix

Excitonic Model Hamiltonians

To further account for the **exciton-vibration couplings**,

$$\hat{H} = \hat{H}_{\text{ex}} + \hat{H}_{\text{vib}} + \hat{H}_{\text{ex-vib}}$$

$$\hat{H}_{\text{ex}} = \sum_{i=1}^{N_{\text{ex}}} \varepsilon_i \hat{c}_i^\dagger \hat{c}_i + \sum_{i \neq j} V_{ij} \hat{c}_i^\dagger \hat{c}_j$$

$$\hat{H}_{\text{vib}} = \sum_{I=1}^{N_{\text{vib}}} \omega_I \hat{b}_I^\dagger \hat{b}_I$$

$$\hat{H}_{\text{ex-vib}} = \sum_{i,j,I} g_{ij}^{I} \hat{c}_i^\dagger \hat{c}_j \left(\hat{b}_I^\dagger + \hat{b}_I\right) + \sum_{i,j,I,J} g_{ij}^{IJ} \hat{c}_i^\dagger \hat{c}_j \left(\hat{b}_I^\dagger + \hat{b}_I\right)\left(\hat{b}_J^\dagger + \hat{b}_J\right)$$

$N_{\text{ex}} \sim 10^{0-1}$

$N_{\text{vib}} \sim 3 \times N_{\text{atom}} \gg 10^{0-1}$

Challenges:

1. **Model construction: How to build the basis and evaluate the parameters?**
2. **Quantum dynamics: How to simulate strongly correlated systems with large N_{vib} ?**

Basis Selection

Numerical renormalization group (NRG)

K. G. Wilson, *Phys. Rev. B* **1971**, 4, 3174. (1982 Nobel prize in physics)

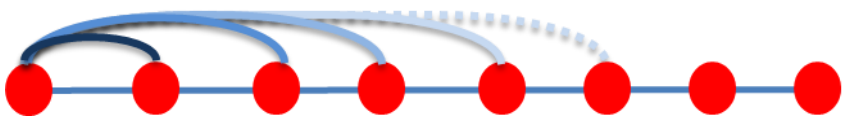

Keep only *M* energetically lowest states

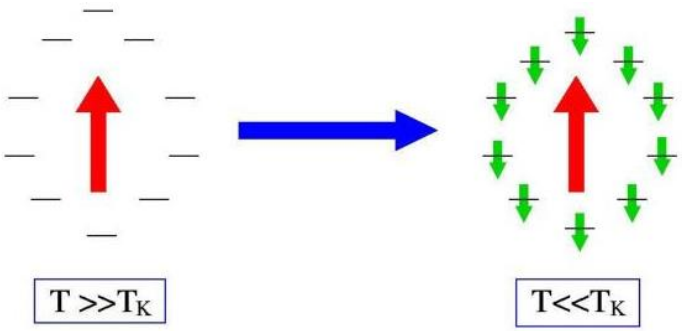

Kondo impurity model

NRG works well in weakly correlated systems, but fails in moderately and strongly correlated systems.

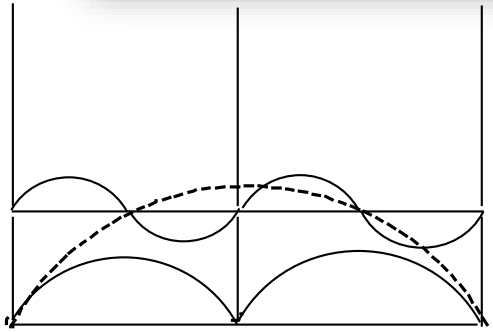

NRG basis describes the inter-subsystem boundaries poorly.

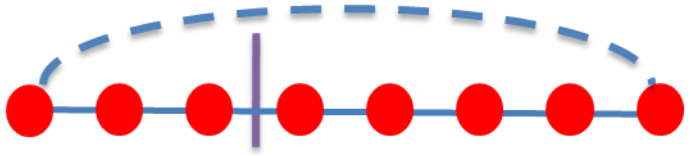

Density Matrix Renormalization Group (DMRG)

S. White, *Phys. Rev. Lett.* **1992**, 69, 2863.

Renormalized Excitonic Model (REM)

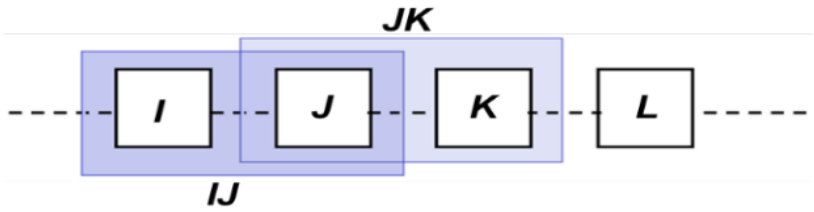

NRG **REM**

M. Al Hajj, J.-P. Malrieu, N. Guihéry, *Phys. Rev. B* **2005**, 72, 224412

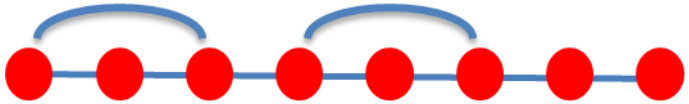

$$\hat{H} = \sum_I \hat{H}_I + \sum_{IJ} \hat{H}_{I-J} + \cdots$$

$$\hat{H}^{\mathrm{REM}} = \sum_I \hat{H}_I^{\mathrm{eff}} + \sum_{IJ} \hat{H}_{I-J}^{\mathrm{eff}} + \cdots$$

Improve the description of inter-fragment interaction
through **Bloch's effective Hamiltonian theory**

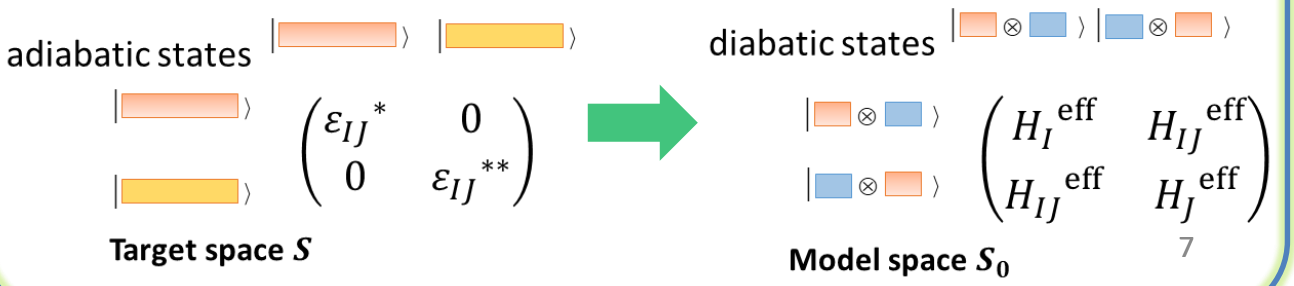

H. Zhang, J. P. Malrieu, **H. Ma**, J. Ma, *J. Computat. Chem.* **2012**, 33, 34.
Y. Ma, Y. Liu, **H. Ma**, *J. Chem. Phys.* **2012**, 136, 224412.

Renormalized Excitonic Model (REM)

Examples:

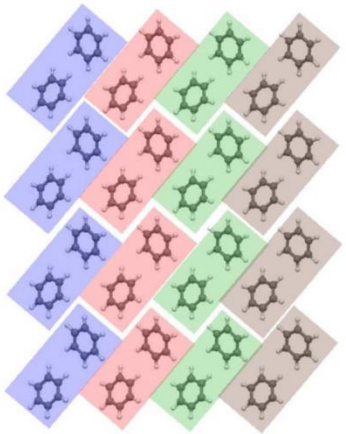

Excitation energy (S_1) in benzene crystal (eV)

system	one-column	two-column	three-column	four-column
REM-TDDFT	5.682	5.664	5.660	5.660
TDDFT	5.685	5.671	5.672	5.672
Δ	−0.003	−0.007	−0.012	−0.012

[a]The LC-BLYP/6-31G is used in the calculations.

Y. Ma, **H. Ma**, *J. Phys. Chem. A* **2013**, 117, 3655.

DOS for charge transfer states in tetracene/PTCDA interface

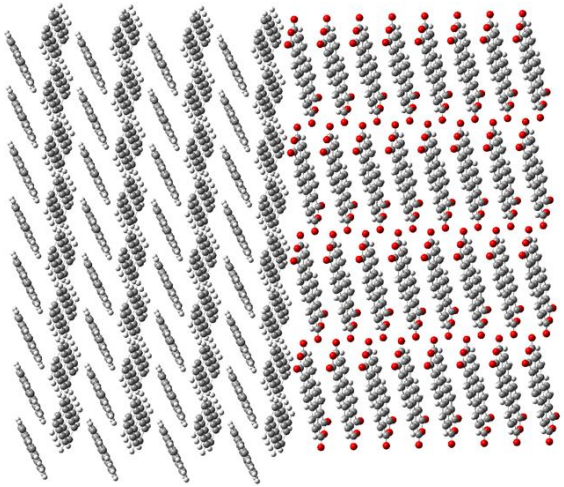

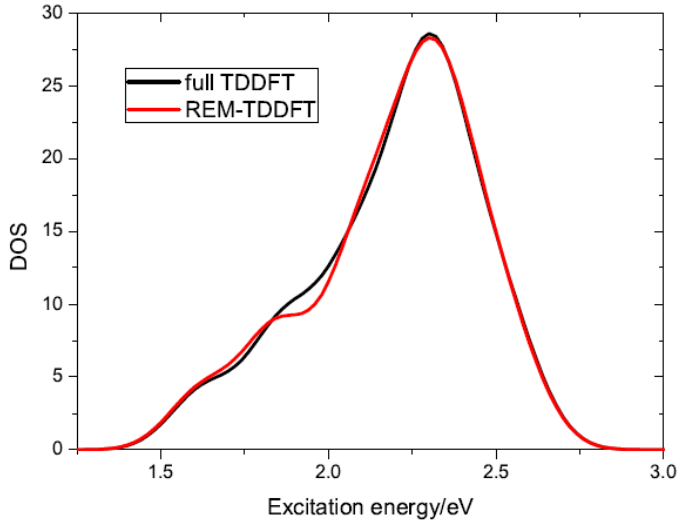

H. Ma, A. Troisi, *Adv. Mater.* **2014**, 26, 6163.

W. Li, **H. Ma**, S. Li, J. Ma, *Chem. Sci.* **2021**, 12, 14987.

Automatic Construction of Excitonic Basis

Using quantum information theory (QIT) to construct excitonic basis (block interaction product state, BIPS) automatically

→Measure system-environment entanglement by the eigenvalues of **reduced density matrix (RDM)**

$$\hat{\rho}_S = Tr_E|\Psi_{SE}\rangle\langle\Psi_{SE}| = \sum_{e\in\mathcal{H}_E}\langle e|\Psi_{SE}\rangle\langle\Psi_{SE}|e\rangle$$

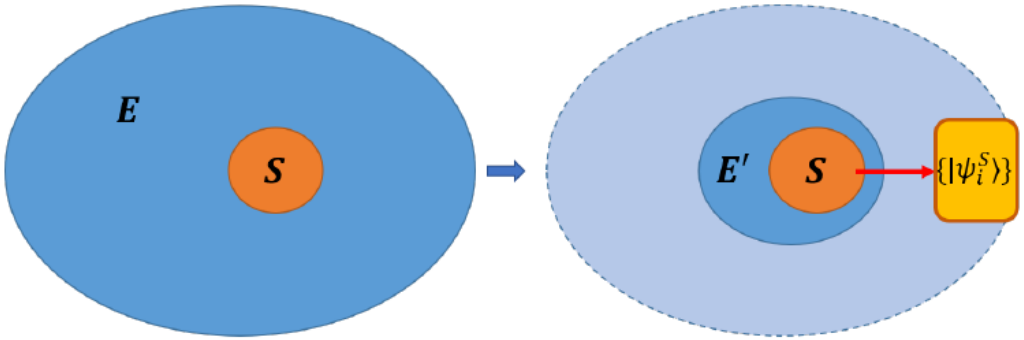

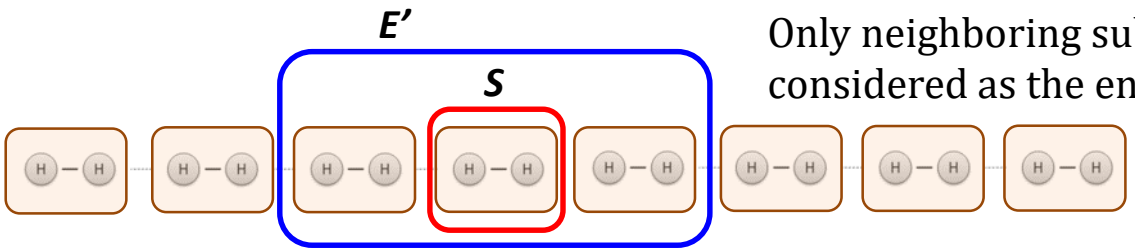

Only neighboring subsystems are considered as the environment.

K. Wang, Z. Xie, Z. Luo, **H. Ma**, *J. Phys. Chem. Lett.* **2022**, 13, 462.

Automatic Construction of Excitonic Basis

➢ **Example: $(H_2)_4$**

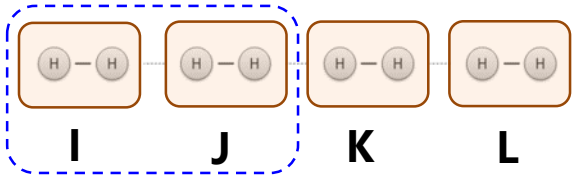

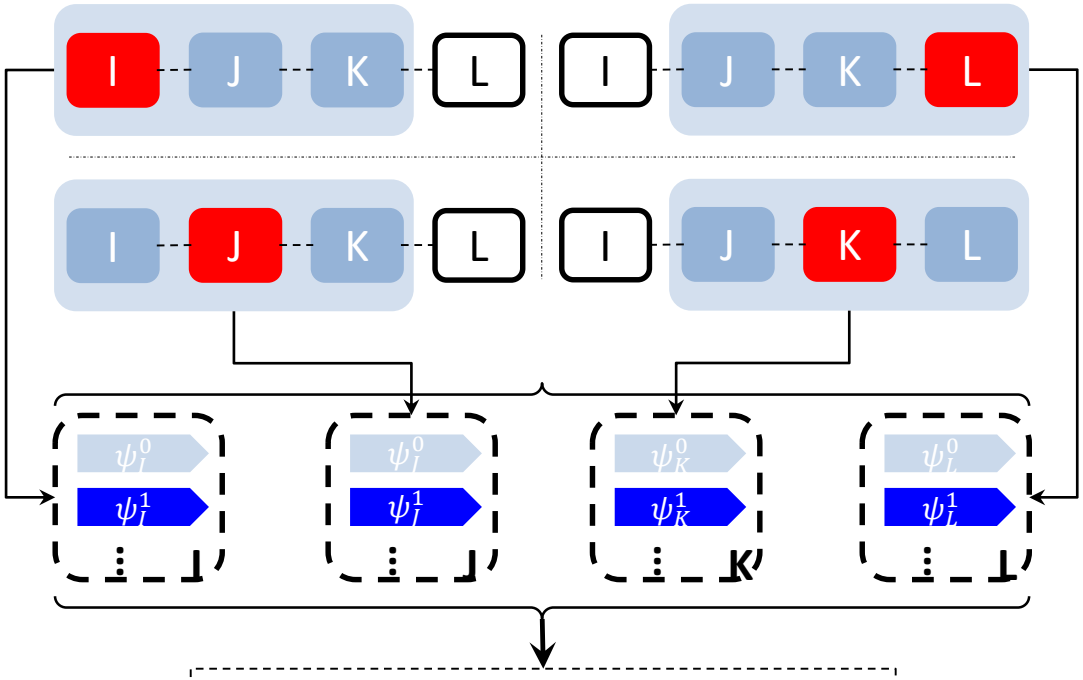

$$\hat{\rho} = |\Psi^*_{IJK}\rangle\langle\Psi^*_{IJK}|$$

$$\hat{\rho}_J = \mathrm{Tr}_{IK}\hat{\rho} = \sum_{n,m} \rho^J_{nm} |n\rangle\langle m|$$

（**Reduce density matrix**）

Only consider Two-body effects !

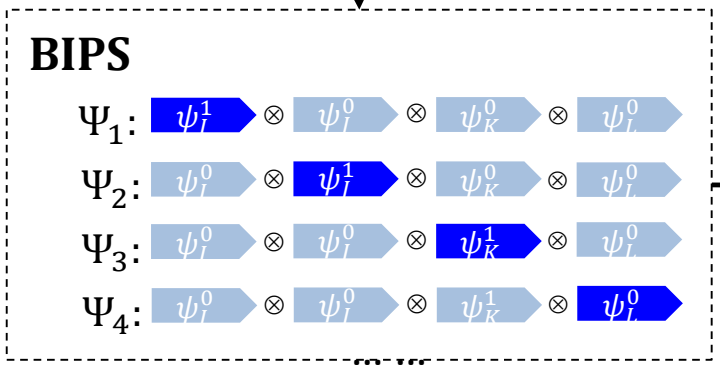

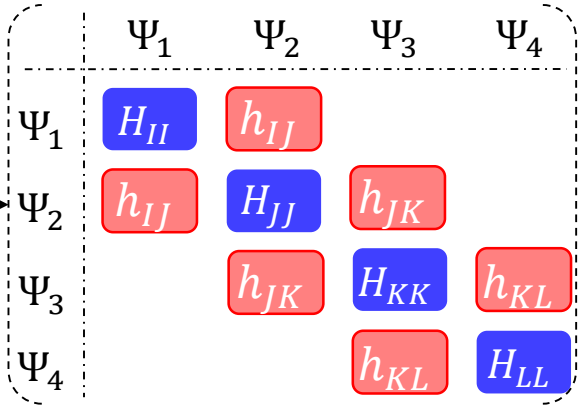

Automatic Construction of Excitonic Basis

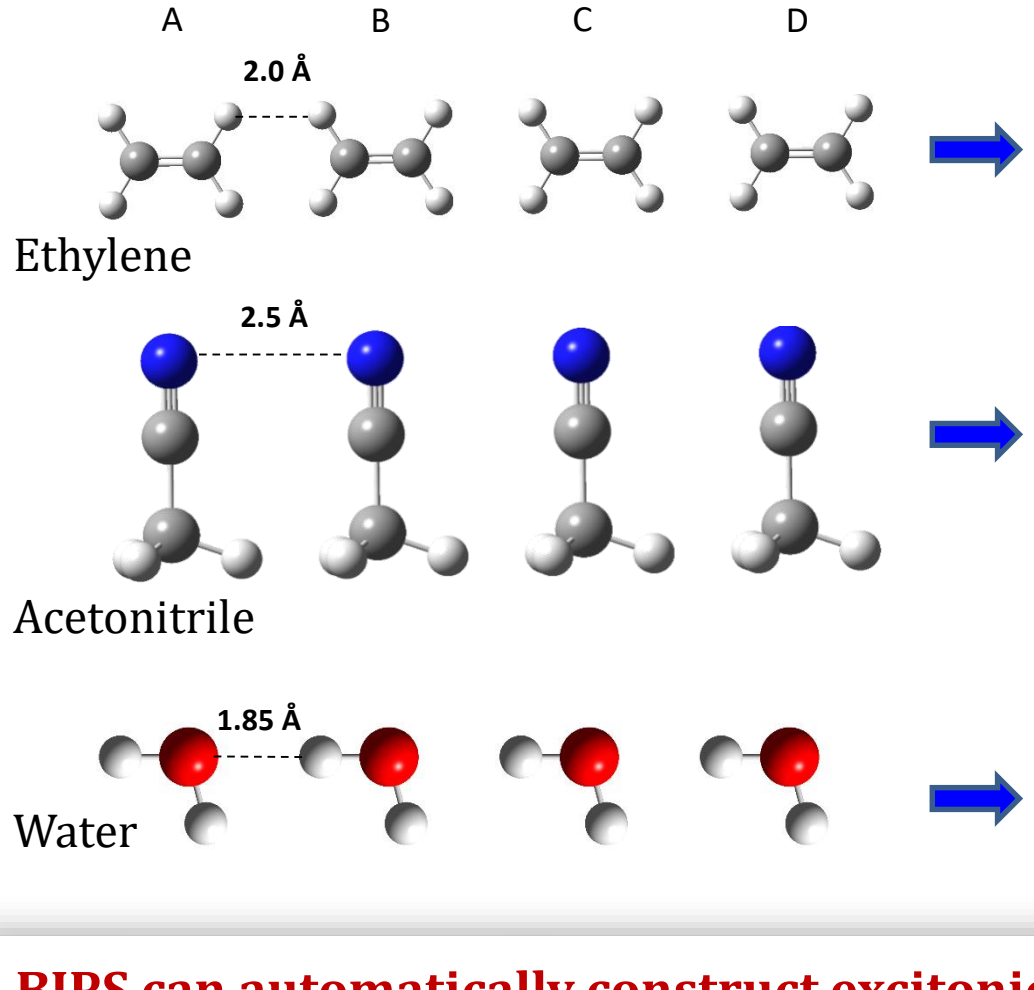

n-BIPSs

$|\psi_A^* \psi_B^0 \psi_C^0 \psi_D^0\rangle$
$|\psi_A^0 \psi_B^* \psi_C^0 \psi_D^0\rangle$
$|\psi_A^0 \psi_B^0 \psi_C^* \psi_D^0\rangle$
$|\psi_A^0 \psi_B^0 \psi_C^0 \psi_D^*\rangle$

c-BIPSs

$|\psi_A^+ \psi_B^- \psi_C^0 \psi_D^0\rangle$
$|\psi_A^0 \psi_B^0 \psi_C^- \psi_D^+\rangle$

$|\psi_A^+ \psi_B^- \psi_C^0 \psi_D^0\rangle$
$|\psi_A^- \psi_B^+ \psi_C^0 \psi_D^0\rangle$
$|\psi_A^0 \psi_B^+ \psi_C^- \psi_D^0\rangle$
$|\psi_A^0 \psi_B^- \psi_C^+ \psi_D^0\rangle$
$|\psi_A^0 \psi_B^0 \psi_C^+ \psi_D^-\rangle$
$|\psi_A^0 \psi_B^0 \psi_C^- \psi_D^+\rangle$

BIPS can automatically construct excitonic bases for different aggregated systems.

K. Wang, Z. Xie, Z. Luo, **H. Ma**, *J. Phys. Chem. Lett.* **2022**, 13, 462.

Automatic Construction of Excitonic Basis

➢ **Example: $(C_6H_6)_n$**

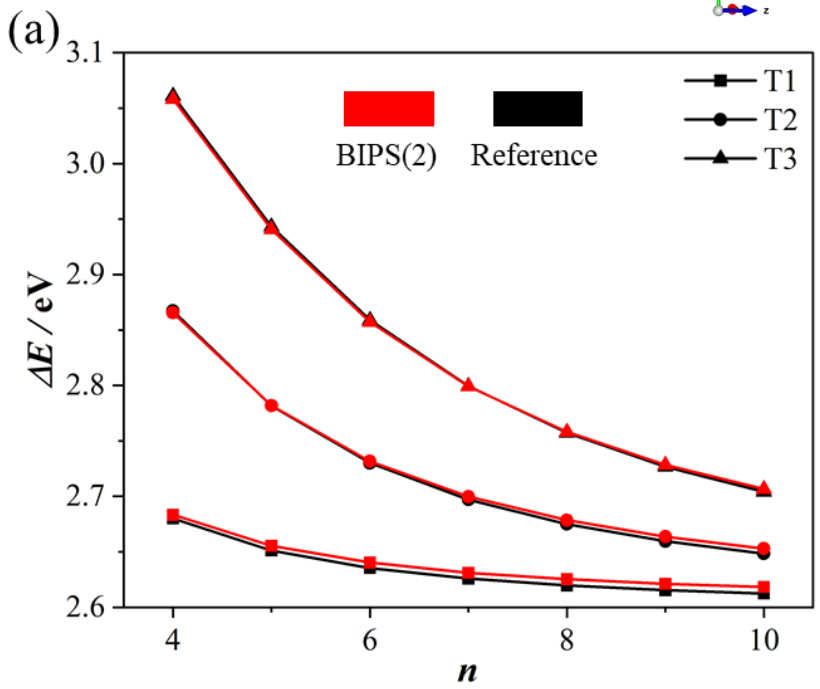

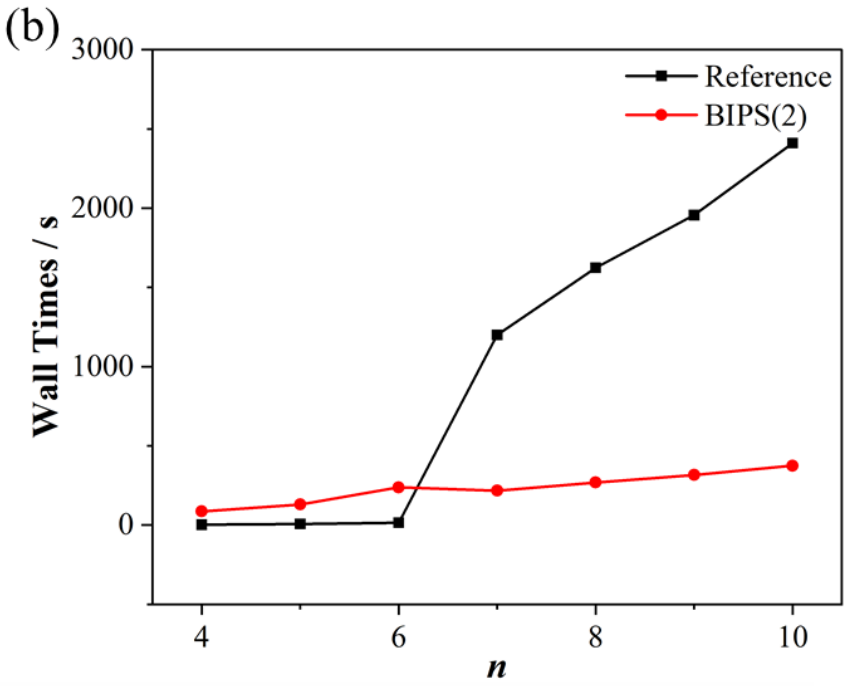

- **BIPS accuracy remains within the maximum deviation of 7 meV.**
- **BIPS exhibits almost linear growth in time consumption.**

K. Wang, Z. Xie, Z. Luo, **H. Ma**, *J. Phys. Chem. Lett.* **2022**, 13, 462.

Automatic Construction of Excitonic Basis

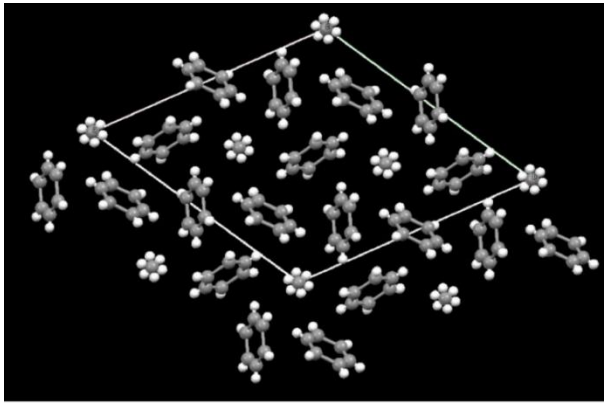

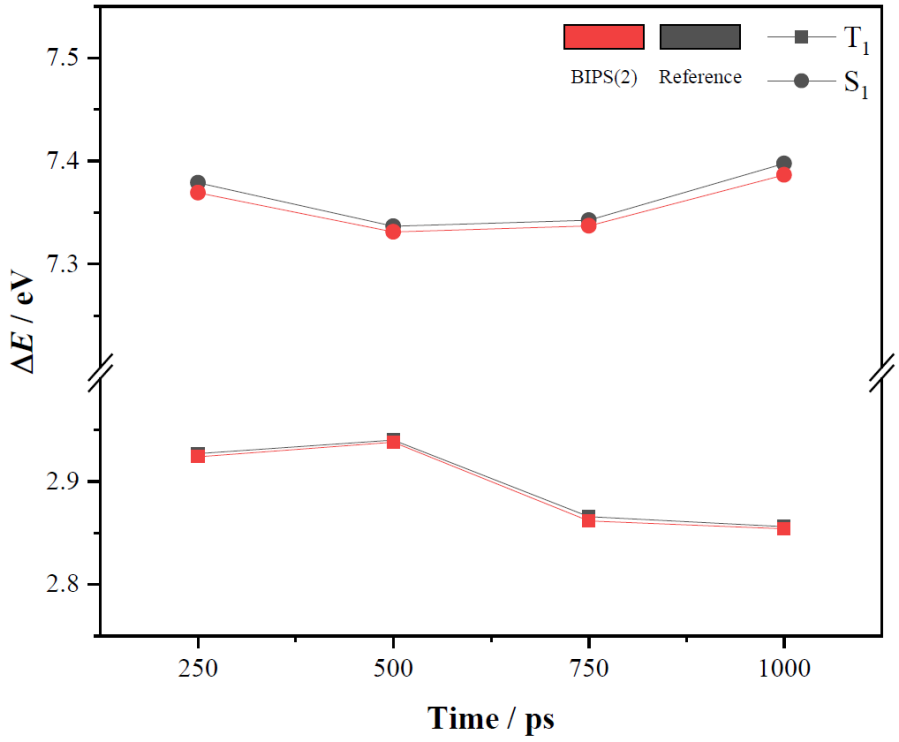

BIPS can correctly mimic the energetic fluctuations under different distorted geometries.

Automatic Construction of Excitonic Basis

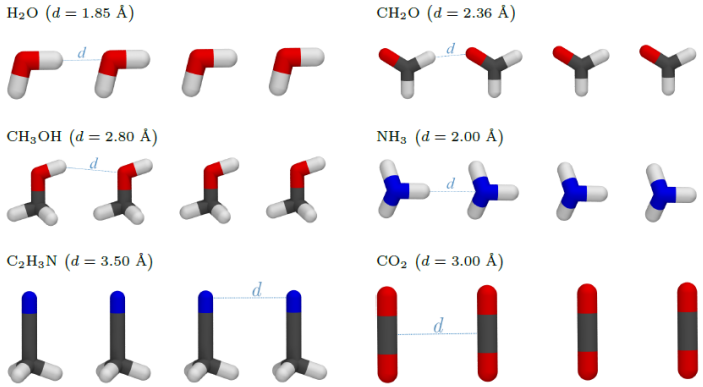

$$\mu = \langle \Psi^* | \sum_i q_i \hat{\boldsymbol{r}}_i | \Psi^* \rangle$$

$$\mu^{\mathrm{T}} = \langle \Psi^0 | \sum_i q_i \hat{\boldsymbol{r}}_i | \Psi^* \rangle$$

	ΔE / eV		μ / a.u.		μ^{T} / a.u.	
	Reference	$\delta(3)$	Reference	$\delta(3)$	Reference	$\delta(3)$
$(H_2O)_4$	9.1463	0.0112	2.7817	0.0288	0.3091	0.0307
$(CH_2O)_4$	4.5691	0.0286	4.5822	0.0071	0.0014	0.0006
$(CH_3OH)_4$	8.4042	0.0094	2.6123	0.0006	0.0415	0.0069
$(NH_3)_4$	7.9446	0.0120	1.8979	0.0062	0.6309	0.0107
$(C_2H_3N)_4$	7.6922	0.0260	5.4202	0.0098	0.0074	0.0033
$(CO_2)_4$	9.6696	0.0065	0.0001	0.0001	0.0000	0.0000

BIPS provides accurate descriptions for both excitation energies and first-order wave function properties.

K. Wang, Z. Xie, Z. Luo, **H. Ma**, *J. Phys. Chem. Lett.* **2022**, 13, 462.

Evaluation of Exciton-Phonon Couplings

Direct scanning under linear approximation

$$g_i^I = \frac{\partial \varepsilon_i}{\partial Q_I}$$

$$g_{ij}^I = \frac{\partial V_{ij}}{\partial Q_I}$$

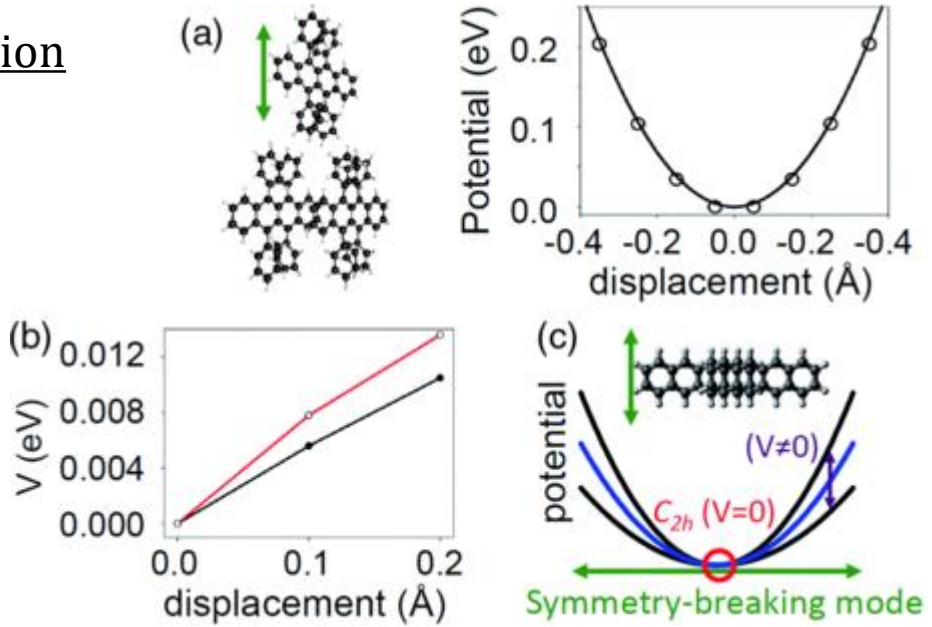

H. Tamura, et al., *Phys. Rev. Lett.* **2015**, 115, 107401.

- Vibration modes in molecule:

$$3N_{\mathbf{atom}} - 6(5)$$

- Phonon modes in crystal:

infinitely many (especially low-frequency ones)

Due to the too many phonon modes in condensed phase, computational costs of direct scanning are unaffordable!

Evaluation of Exciton-Phonon Couplings

Use the locality of electronic structure

$$g_{ij}^{I} = \sum_{a} \frac{\partial V_{ij}}{\partial a} \frac{\partial a}{\partial Q_I} \approx \sum_{\mathbf{a} \in \text{system}} \frac{\partial V_{ij}}{\partial a} \frac{\partial a}{\partial Q_I}$$

$$\Downarrow$$

$$g_{ij}^{I} = \nabla V_{ij} \cdot \mathbf{Q}_I^c$$

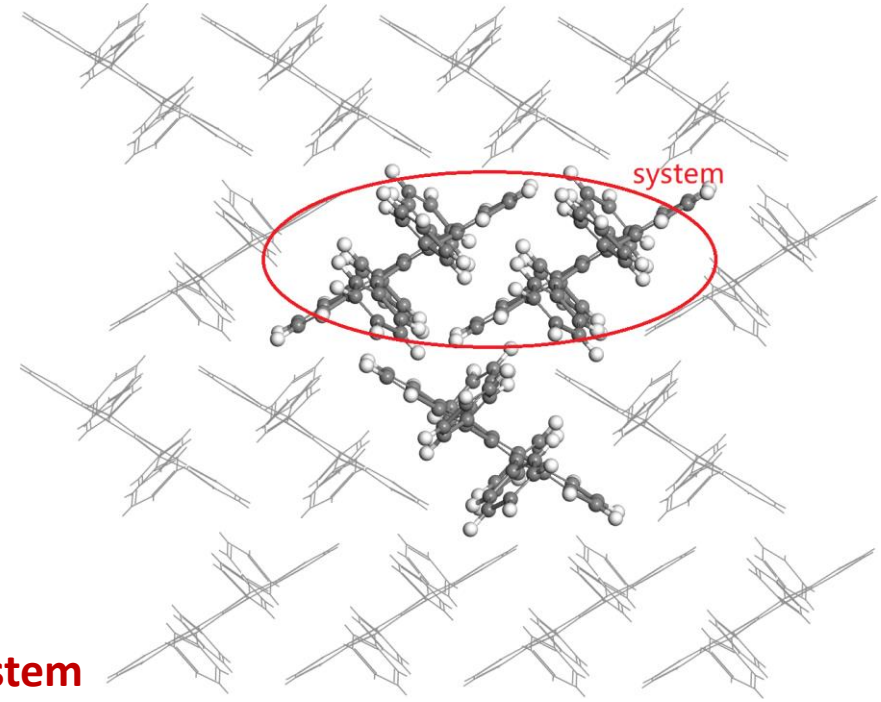

bc plane of rubrene crystal

∇V_{ij}: Quantum chemistry + scanning → **subsystem**

$\boldsymbol{Q}_I^c$: phonon band structure → **crystal**

X. Xie, A. Santana-Bonilla, A. Troisi, *J. Chem. Theory Comput.* **2018,** 14, 3752

Scanning costs: $\infty \rightarrow 3N_{\text{atom}}^{\text{system}}$

X. Xie, A. Santana-Bonilla, W. Fang, C. Liu, A. Troisi, **H. Ma**, *J. Chem. Theory Comput.* **2019,** 15, 3721

Evaluation of Exciton-Phonon Couplings

Example: Non-local ex-ph coupling (CT-TT) of singlet fission (SF) in rubrene

Exp: K. Miyata, et. al. *Nat. Chem.* **2017**, 9, 983.

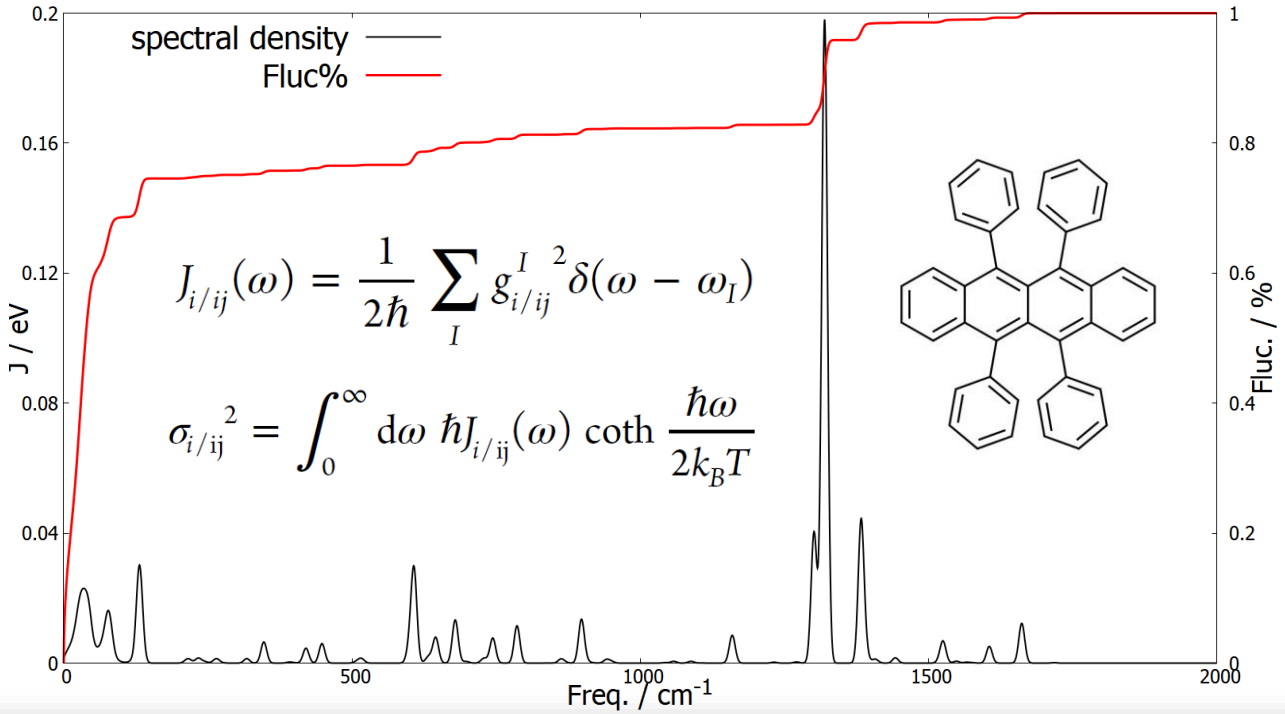

1. **Contribution: Low-frequency > High frequency (T= 300 K)**
2. **Crystal environment is important for SF in rubrene**

X. Xie, A. Santana-Bonilla, W. Fang, C. Liu, A. Troisi, **H. Ma**, *J. Chem. Theory Comput.* **2019,** 15, 3721

Outline

- Background: Exciton dynamics

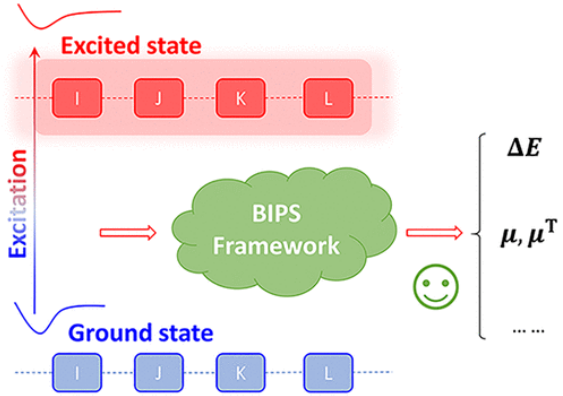

- Model construction
  - Automatic construction of excitonic basis
  - Evaluation of exciton-phonon couplings

- **Quantum dynamics simulation**
  - **Time-dependent density matrix renormalization group (TD-DMRG)**
  - **Stochastic adaptive single-site TD-DMRG**

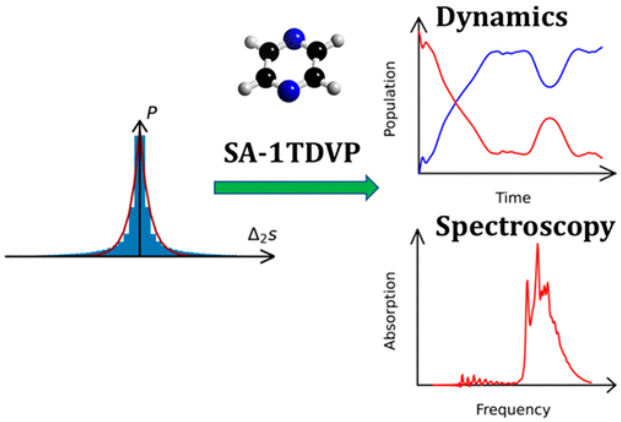

Matrix Product State (MPS)

Decomposition of high-rank tensor

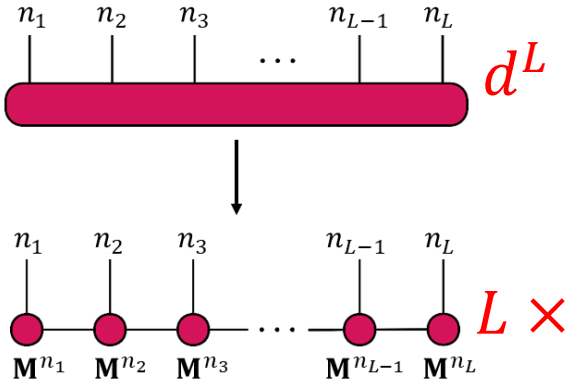

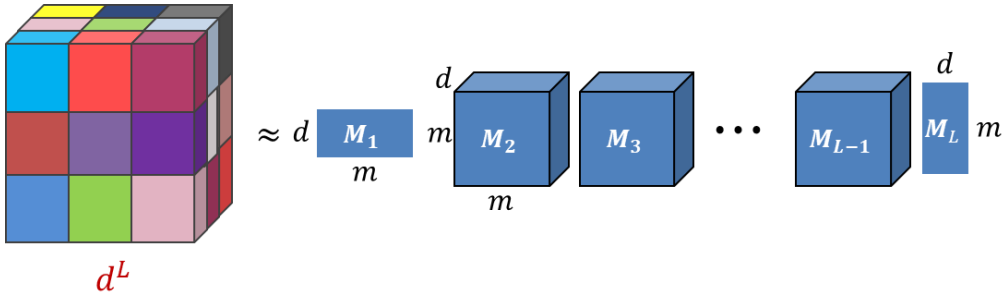

Compressibility, **locality**

MPS: $$|\psi\rangle = \sum_{n_1 \cdots n_L} \mathbf{M}_1^{n_1} \mathbf{M}_2^{n_2} \cdots \mathbf{M}_L^{n_L} |n_1, n_2, \cdots, n_L\rangle$$

Density Matrix Renormalization Group (DMRG)

optimize **M** matrices iteratively

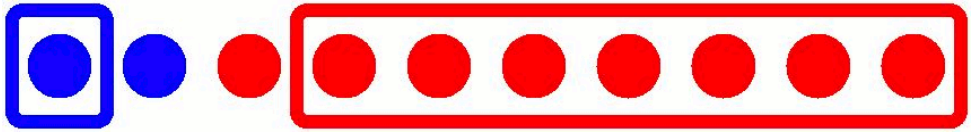

S. White, *Phys. Rev. Lett.* **1992**, 69, 2863.
U. Schollwöck, *Rev. Mod. Phys.* **2005**, 77, 259.

Time-Dependent DMRG (TD-DMRG)

DMRG

S. White, *Phys. Rev. Lett.* **1992**, 69, 2863.
U. Schollwöck, *Rev. Mod. Phys.* **2005**, 77, 259.

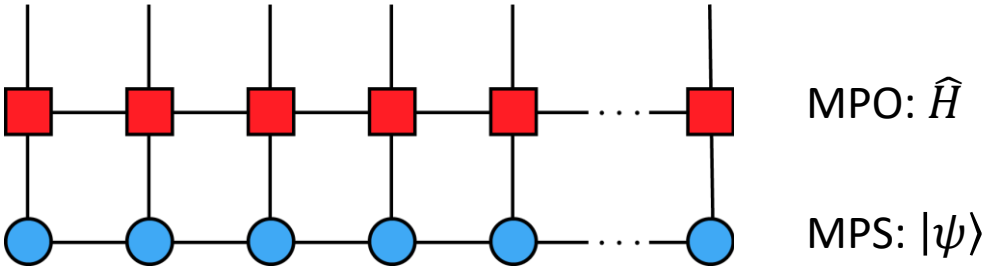

TD-DMRG

M. A. Cazalilla, J. B. Marston, *Phys. Rev. Lett.* **2002**, 88, 256403.
H. Luo, T. Xiang, X. Wang, *Phys. Rev. Lett.* **2003**, 91, 049701.

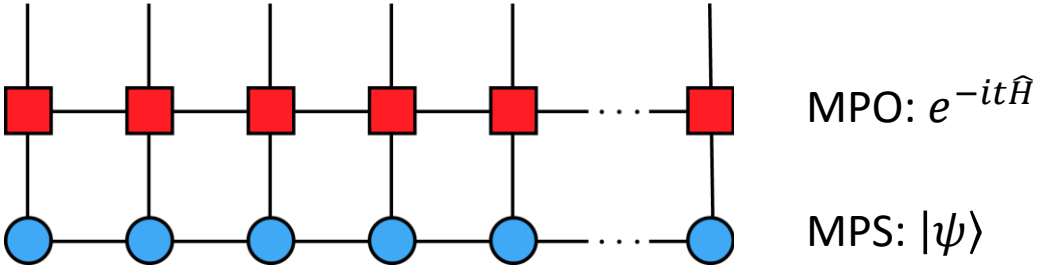

How to construct $e^{-it\hat{H}}$ efficiently and accurately?

Time-Dependent DMRG (TD-DMRG)

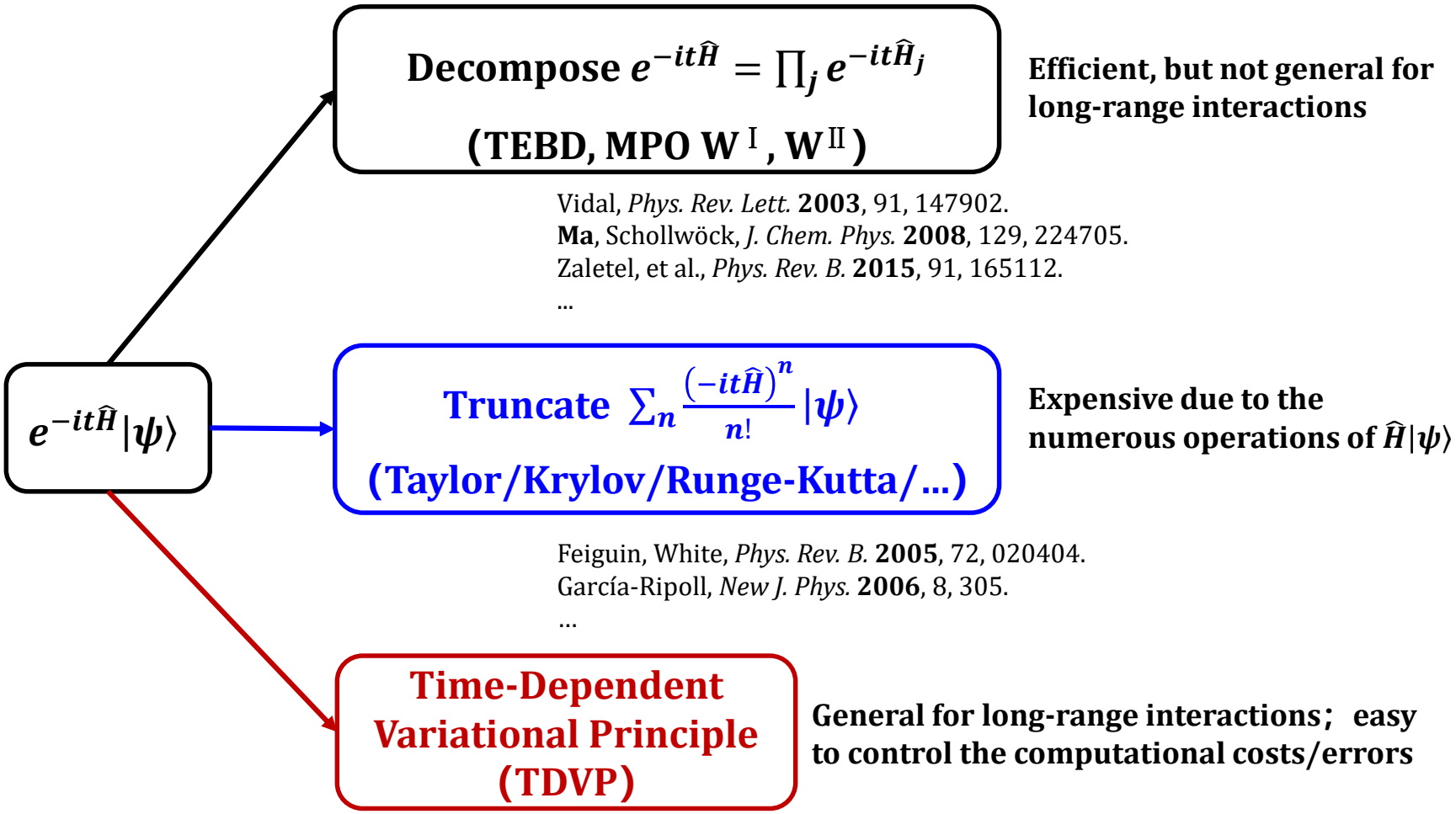

Vidal, *Phys. Rev. Lett.* **2003**, 91, 147902.
Ma, Schollwöck, *J. Chem. Phys.* **2008**, 129, 224705.
Zaletel, et al., *Phys. Rev. B.* **2015**, 91, 165112.
...

Feiguin, White, *Phys. Rev. B.* **2005**, 72, 020404.
García-Ripoll, *New J. Phys.* **2006**, 8, 305.
...

Haegeman, et al., *Phys. Rev. Lett.* **2011**, 107, 070601.
Haegeman, et al., *Phys. Rev. B* **2016**, 94, 165116.

Reviews: Paeckel, et al., *Ann. Phys.* **2019**, 411, 167998.
Ren, Li, Jiang, Wang, Shuai, *WIREs ComputMol Sci.* **2022**, doi: 10.1002/wcms.1614.

Time-Dependent Variational Principle (TDVP)

Time evolution → **variational optimization**

$$\hat{H}|\psi(t)\rangle = i\hbar\frac{\partial}{\partial t}|\psi(t)\rangle$$

$$\text{Minimize } \|\hat{H}|\psi(t)\rangle - \mathrm{i}\hbar\frac{\partial}{\partial t}|\psi(t)\rangle\|^2$$

optimize the basis in which truncated space?

Tangent space

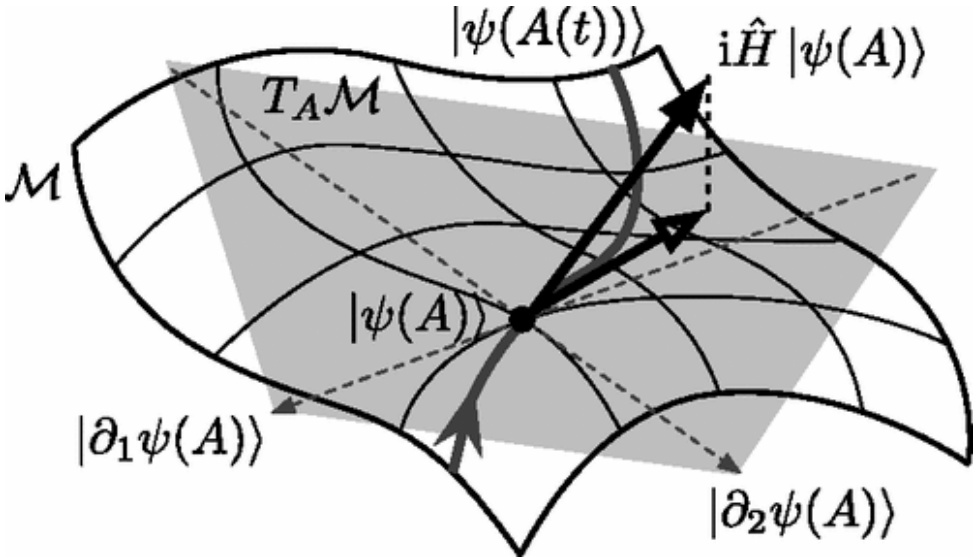

$\hat{P}_T$ is called **tangent space projection operator**, which can project the wave function into the space defined by $\frac{\partial\psi}{\partial M_j}$.

(full: $d^L \rightarrow$ projection: dD^2)

The final evolution function:

$$i\hbar\frac{\partial}{\partial t}|\psi(t)\rangle = \hat{P}_T\,\hat{H}|\psi(t)\rangle$$

Haegeman, et al., *Phys. Rev. Lett.* **2011**, 107, 070601.
Haegeman, et al., *Phys. Rev. B* **2016**, 94, 165116.

Time-Dependent Variational Principle (TDVP)

$\hat{P}_T$ in the MPS language (**one-site algorithm**):

$$\hat{P}_T = \sum_{j=1}^{n} \hat{P}_{j-1}^{L} \otimes \hat{I}_j \otimes \hat{P}_{j+1}^{R} - \sum_{j=1}^{n-1} \hat{P}_j^{L} \otimes \hat{P}_{j+1}^{R}$$

Single time step

= *n* steps of forward evolution

+ *n*-1 steps of backward evolution

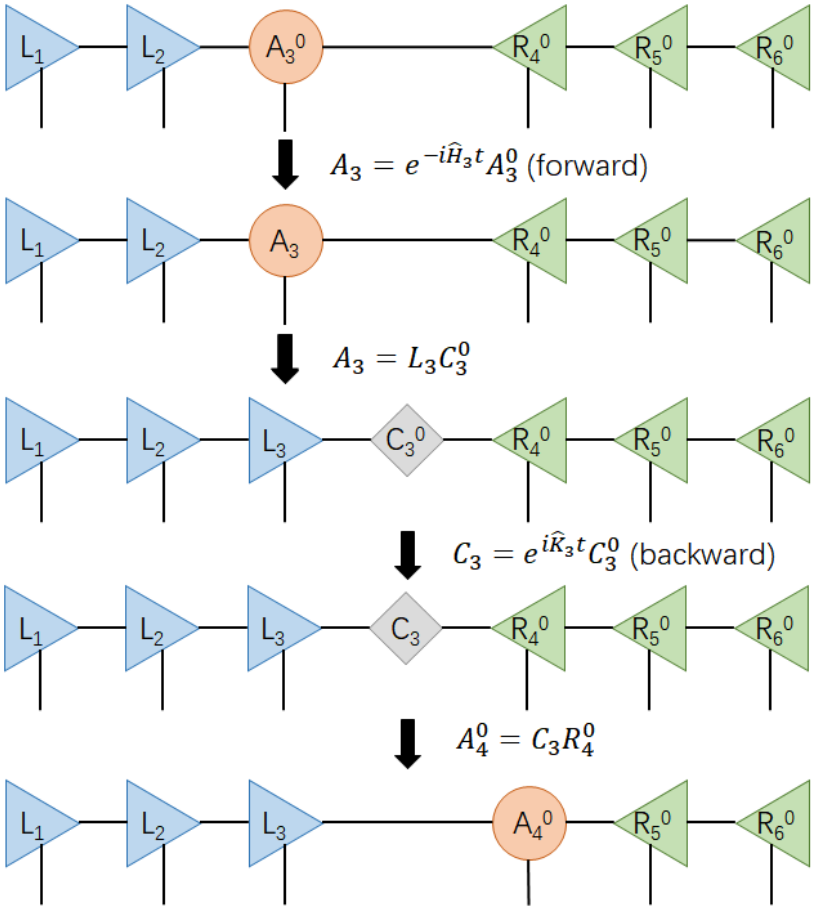

$$|\psi\rangle = \sum_{n_1 \cdots n_L} \mathbf{M}_1^{n_1} \mathbf{M}_2^{n_2} \cdots \mathbf{M}_L^{n_L} |n_1, n_2, \cdots, n_L\rangle$$

Single-Site vs. Two-Site

$\hat{P}_T$ **(two-site algorithm)**

$$\hat{P}_T = \sum_{j=1}^{n-1} \hat{P}_{j-1}^{L} \otimes \hat{I}_j \otimes \hat{I}_{j+1} \otimes \hat{P}_{j+2}^{R} - \sum_{j=1}^{n-2} \hat{P}_j^{L} \otimes \hat{I}_{j+1} \otimes \hat{P}_{j+2}^{R}$$

1TDVP:
update one site
at each step

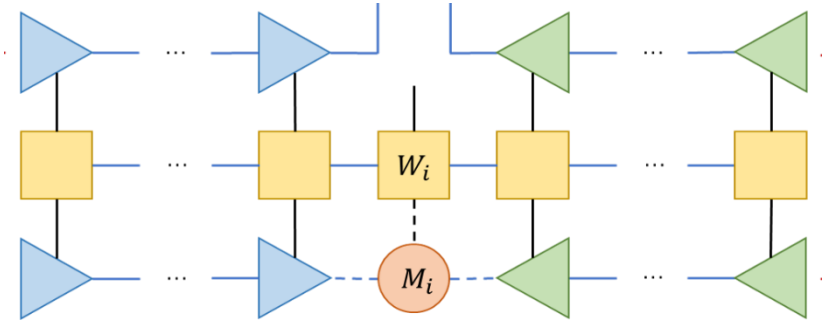

2TDVP:
update two sites
at each step

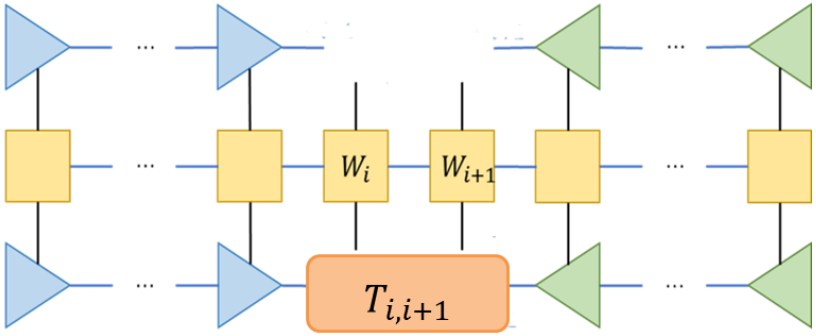

1TDVP vs. 2TDVP

Test of efficiency and accuracy (model: the 4-mode pyrazine)

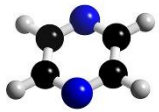

$$\hat{H}_{\text{ex}} = \sum_i \varepsilon_i \hat{c}_i^\dagger \hat{c}_i + \sum_{i \neq j} V_{ij} \hat{c}_i^\dagger \hat{c}_j$$

$$\hat{H}_{\text{vib}} = \sum_{I=1}^{N_{\text{vib}}} \omega_I \hat{b}_I^\dagger \hat{b}_I$$

$$\hat{H}_{\text{ex-vib}} = \sum_{i,j,I} g_{ij}^I \hat{c}_i^\dagger \hat{c}_j (\hat{b}_I^\dagger + \hat{b}_I)$$

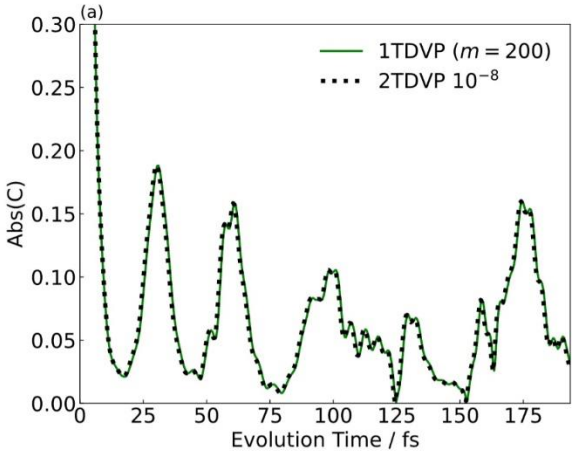

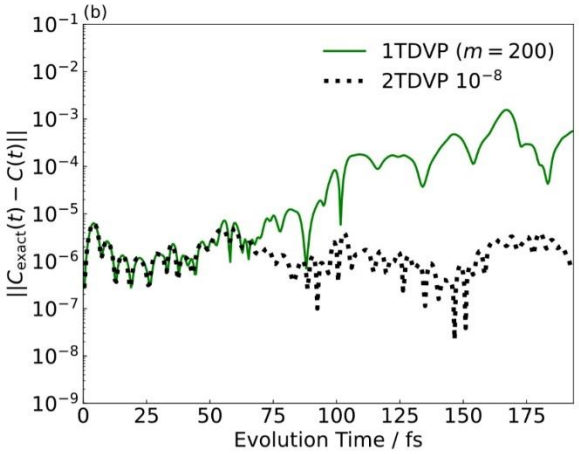

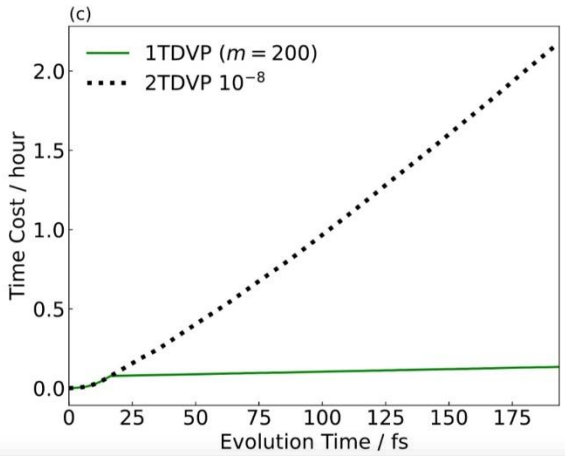

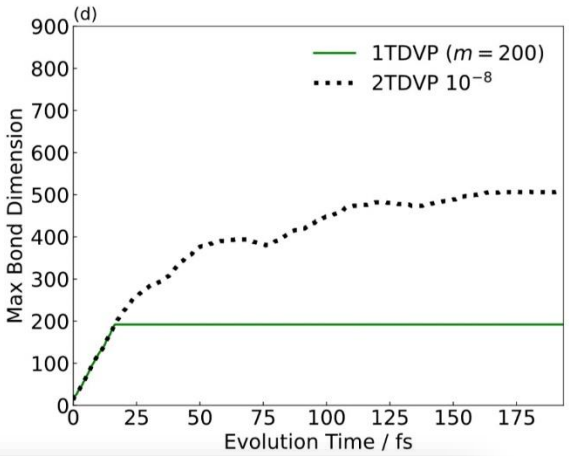

1TDVP is faster, but its error is uncontrollable at long time limit.

Entanglement Growth during Time Evolution

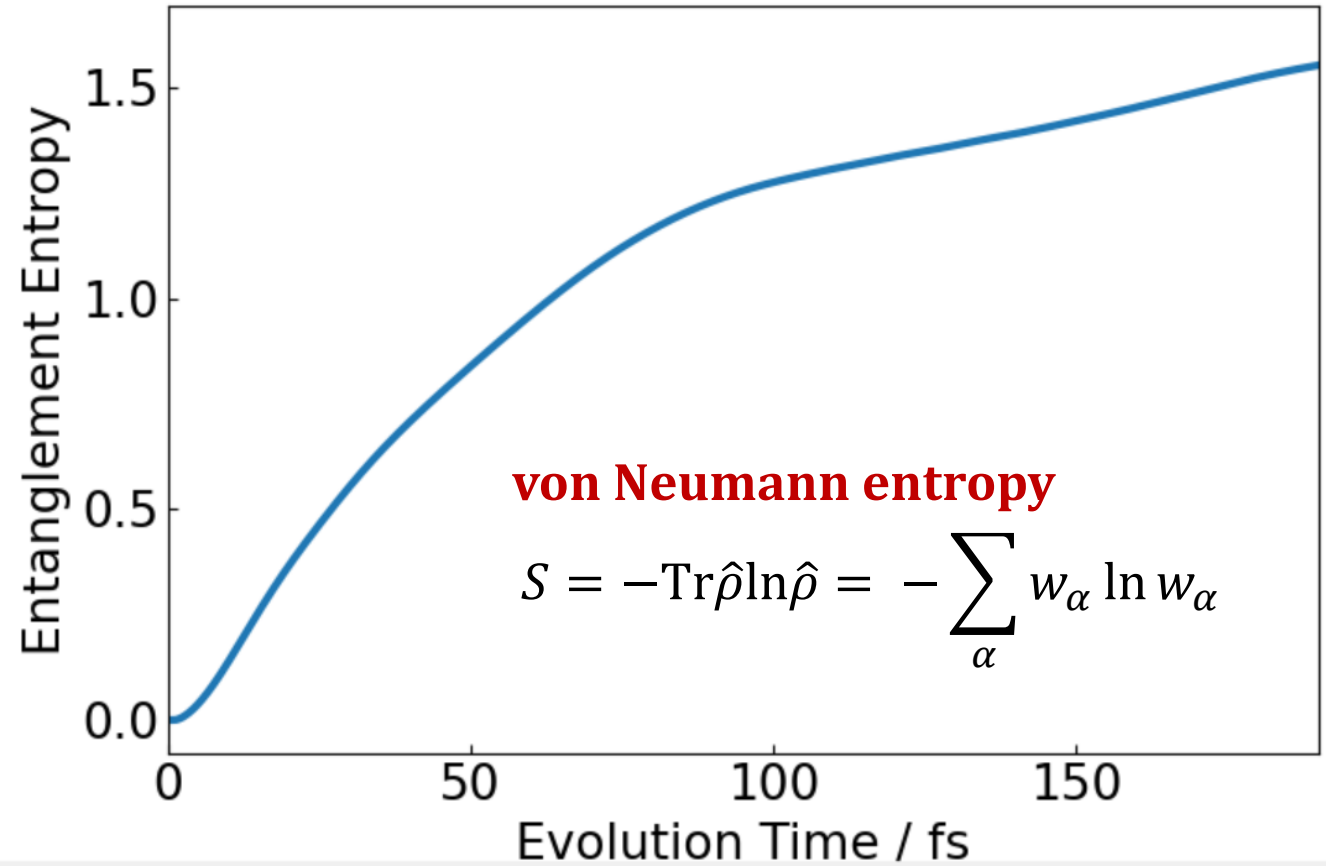

von Neumann entropy

$$S = -\mathrm{Tr}\hat{\rho}\ln\hat{\rho} = -\sum_{\alpha} w_\alpha \ln w_\alpha$$

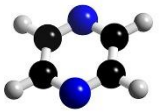

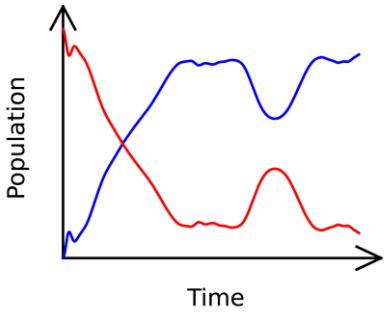

The entanglement grows as time evolves, so the adaptive increasing of *m* in MPS is needed.

1TDVP vs 2TDVP

1TDVP

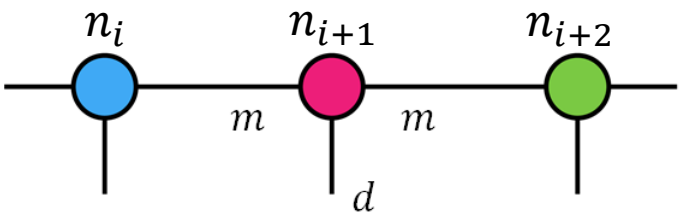

2TDVP

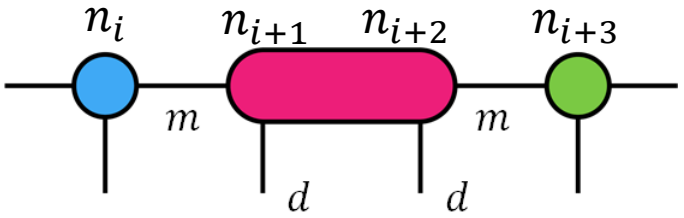

	1TDVP	2TDVP
Variational space	$m \times d \times m$	$m \times d \times d \times m$
Efficiency	high	low
Increase m ?	No (**m non-zero singular values at most**)	Yes (**$m \times d$ non-zero singular values at most**)

(1)

(2) How to set the m or make m increase automatically in 1TDVP?

Xie, Liu, Yao, Schollwöck, Liu, **Ma**, *J. Chem. Phys.* **2019**, 151, 224101.

New adaptive 1TDVP method is needed.

Adaptive 1TDVP

Global treatment

Yang, White, *Phys. Rev. B* **2020**, 102, 094315.

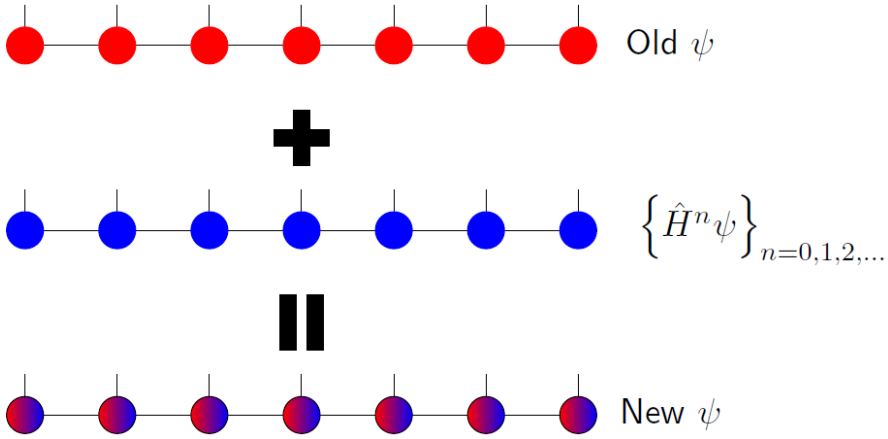

Extend the space through MPS addition

Local treatment

Dunnett, Chin, *Phys. Rev. B* **2021**, 104, 214302.

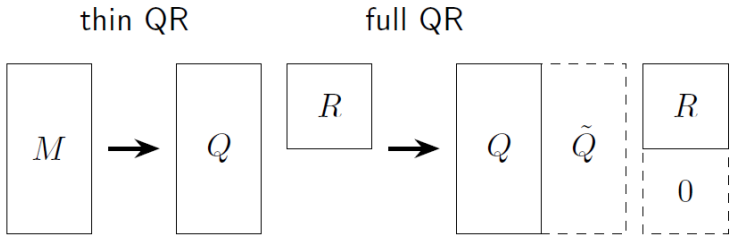

Measure function: $f_j = \|H_{\text{eff},j}A_j\|^2 - \|K_{\text{eff},j}C_j\|^2 + \|H_{\text{eff},j+1}M_{j+1}\|^2$

Extend the space through full QR and converge by calculating the measure function

Both need additional expensive $\hat{H}|\psi\rangle$ operations.

Statistical Distribution of Singular Values in TD-DMRG

$$\lambda_n \sim \exp(\text{const} \times \ln^2 n)$$

Okunishi, Hieida, Akutsu, *Phys. Rev. E* **1999**, 59, R6227.
Chan, Ayers, Croot, *J. Stat. Phys.* **2002**, 109, 289.

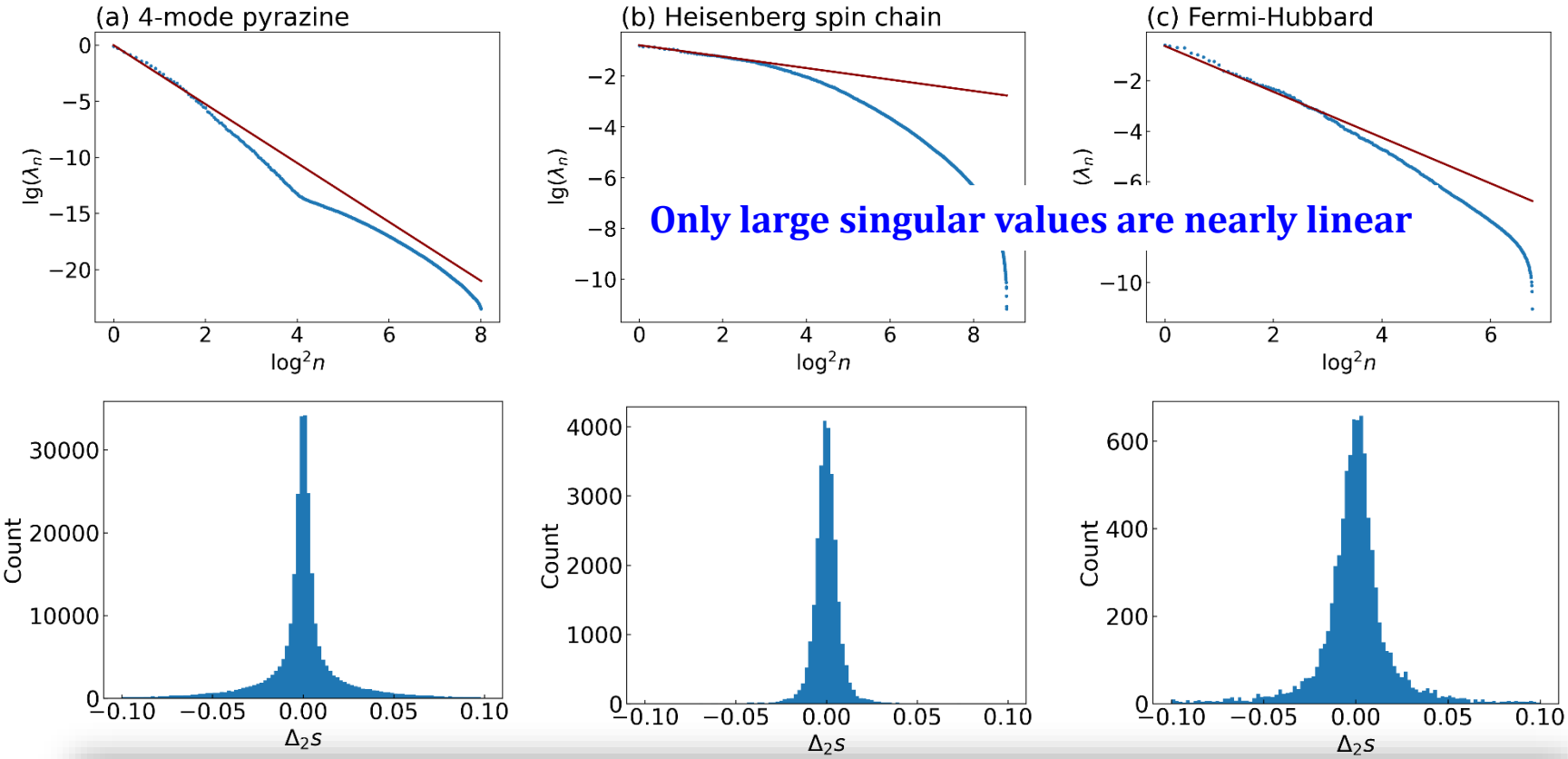

Only large singular values are nearly linear

Distributions of 2nd order singular value logarithms show similar features in different models. (exponential? Gaussian?)

Xu, Xie, Xie, Schollwöck, **Ma**, *JACS Au* **2022**, 2, 335.

Derivation of exponential distribution

Poisson process:

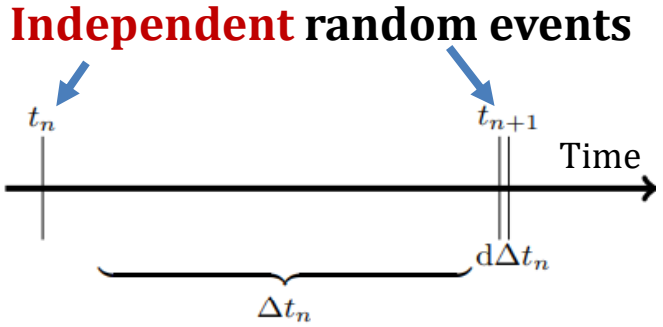

Distribution of singular value logarithms ($s_n = \log\lambda_n$):

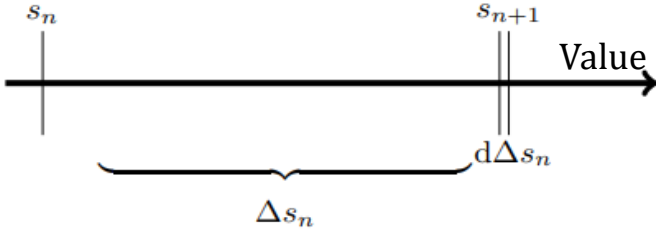

$$P(\Delta s_n) = \beta e^{-\beta \Delta s_n}$$

$$P(\Delta s_{n+1}) = \beta e^{-\beta \Delta s_{n+1}}$$

For $\Delta_2 s = \Delta s_{n+1} - \Delta s_n$

$$P(\Delta_2 s)d(\Delta_2 s) = \int_0^{+\infty} d(\Delta s_n) \int_0^{+\infty\prime} d(\Delta s_{n+1})\, \beta^2 e^{-\beta \Delta s_n} e^{-\beta \Delta s_{n+1}}$$

$$= \int_{\max(0,\Delta_2 s)}^{+\infty} d(\Delta s_n) \beta^2 e^{-\beta \Delta s_n} e^{-\beta(\Delta_2 s + \Delta s_n)} d(\Delta_2 s)$$

$$P(\Delta_2 s) = \frac{\beta}{2} \exp(-\beta |\Delta_2 s|)$$

Random Matrix Theory (RMT): Coupled random events

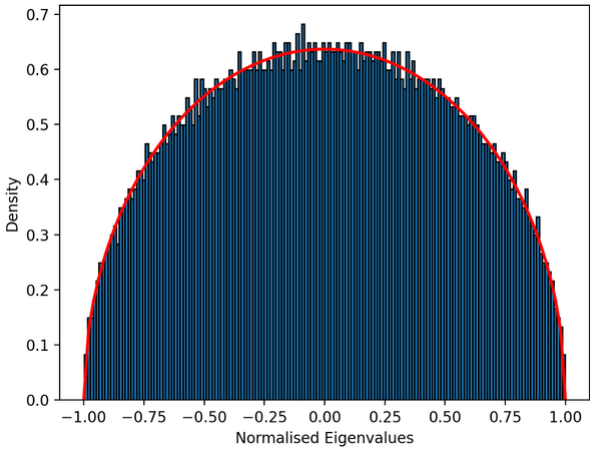

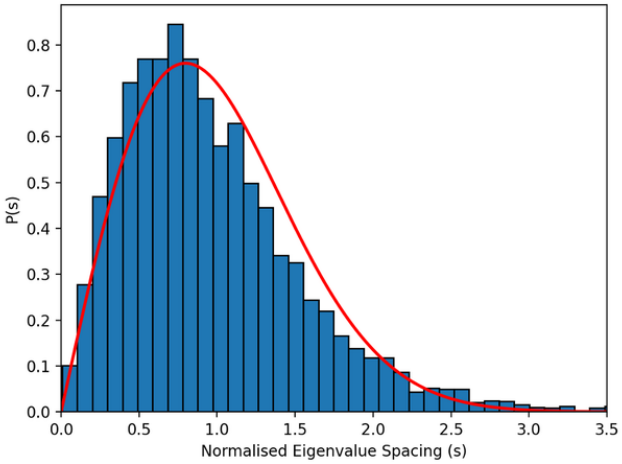

Random matrix | distribution of eigenvalues | distribution of level spacings

Wigner surmise: $P(\Delta s) = \Delta s e^{-\frac{1}{2}(\Delta s)^2}$

E. P. Wigner, *Ann. Math.* **1955**, 62, 548; **1958**, 67, 325.

Derivation of Quasi-Gaussian distribution

For level spacing Δs_n in RMT, **Wigner surmise** gives:

$$\mathrm{P}(\Delta s_n) = \beta \Delta s_n e^{-\frac{\beta}{2}(\Delta s_n)^2}$$

one can derive the distribution of 2nd order gradients:

$$\mathrm{P}(\Delta_2 s)\mathrm{d}(\Delta_2 s) = \beta^2 \int_0^{+\infty} \mathrm{d}(\Delta s_n) \int_0^{+\infty} \mathrm{d}(\Delta s_{n+1})\, \Delta s_n \Delta s_{n+1} e^{-\frac{\beta}{2}(\Delta s_n)^2} e^{-\frac{\beta}{2}(\Delta s_{n+1})^2}$$

$$= \beta^2 \mathrm{d}(\Delta_2 s) \int_0^{+\infty} \mathrm{d}(\Delta s_n) \Delta s_n (\Delta s_n + \Delta_2 s) e^{-\frac{\beta}{2}(\Delta s_n)^2} e^{-\frac{\beta}{2}(\Delta s_n + \Delta_2 s)^2}$$

$$= \beta^2 \mathrm{d}(\Delta_2 s) e^{-\frac{\beta}{4}(\Delta_2 s)^2} \int_{\frac{\Delta_2 s}{2}}^{+\infty} \mathrm{d}y \left[y^2 - \left(\frac{\Delta_2 s}{2} \right)^2 \right] e^{-\beta y^2}$$

$$P(\Delta_2 s) = \beta^2 e^{-\frac{\beta}{4}(\Delta_2 s)^2} \int_{\frac{\Delta_2 s}{2}}^{+\infty} \mathrm{d}y \left[y^2 - \left(\frac{\Delta_2 s}{2} \right)^2 \right] e^{-\beta y^2}$$

Stochastic Adaptive 1TDVP (SA-1TDVP)

Idea:

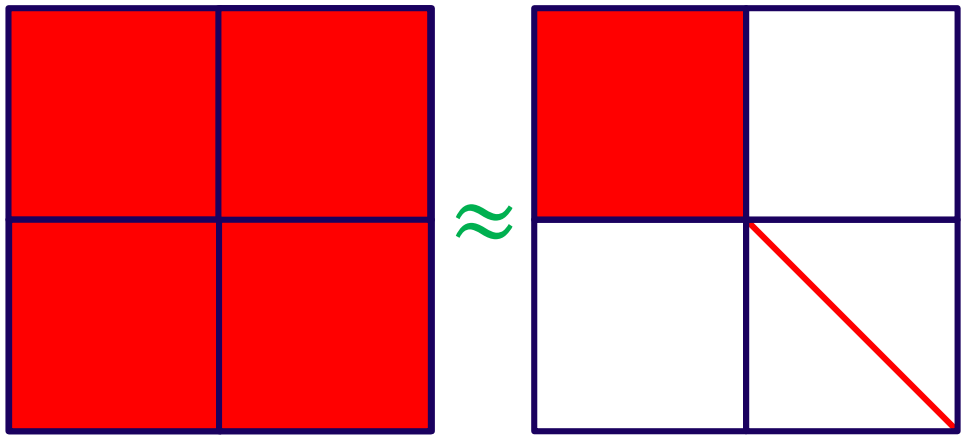

Poisson distribution
(**Independent** random events)

$$P(\Delta s_n) = \beta e^{-\beta \Delta s_n}$$

Wigner surmise
(**Coupled** random events)

$$P(\Delta s_n) = \beta \Delta s_n e^{-\frac{\beta}{2}(\Delta s_n)^2}$$

Matrix diagonalization (large)≈Matrix diagonalization (small) + prediction of other small eigenvalues by stochastic methods

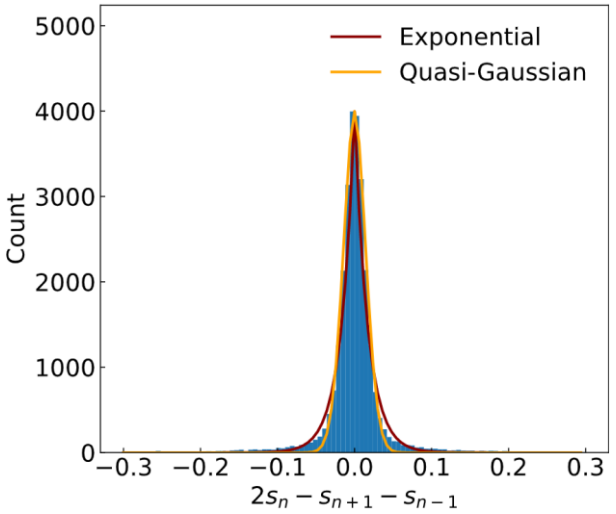

Xu, Xie, Xie, Schollwöck, **Ma**, *JACS Au* **2022**, 2, 335.

Stochastic Adaptive 1TDVP (SA-1TDVP)

Algorithm:

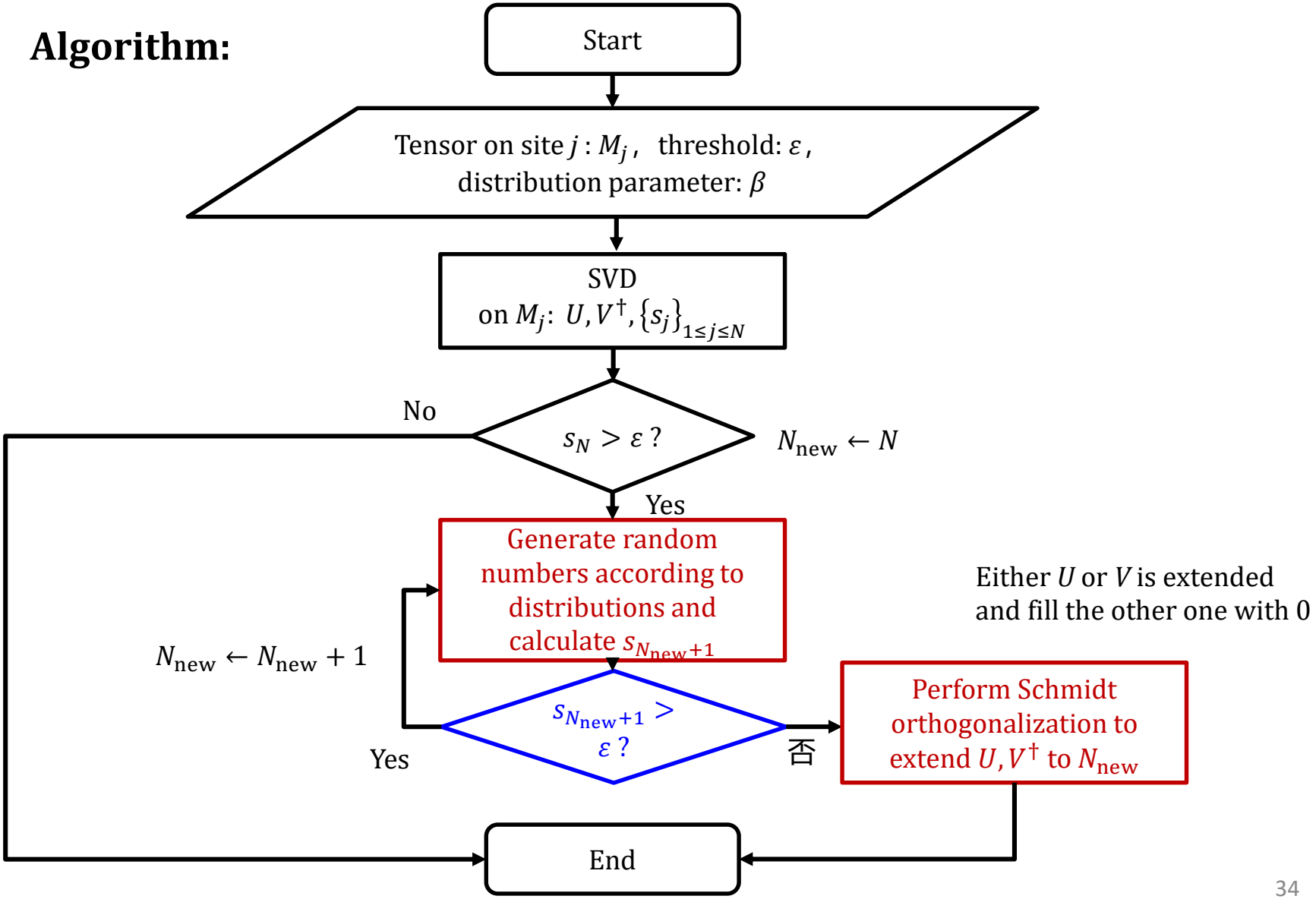

SA-1TDVP

4-mode pyrazine

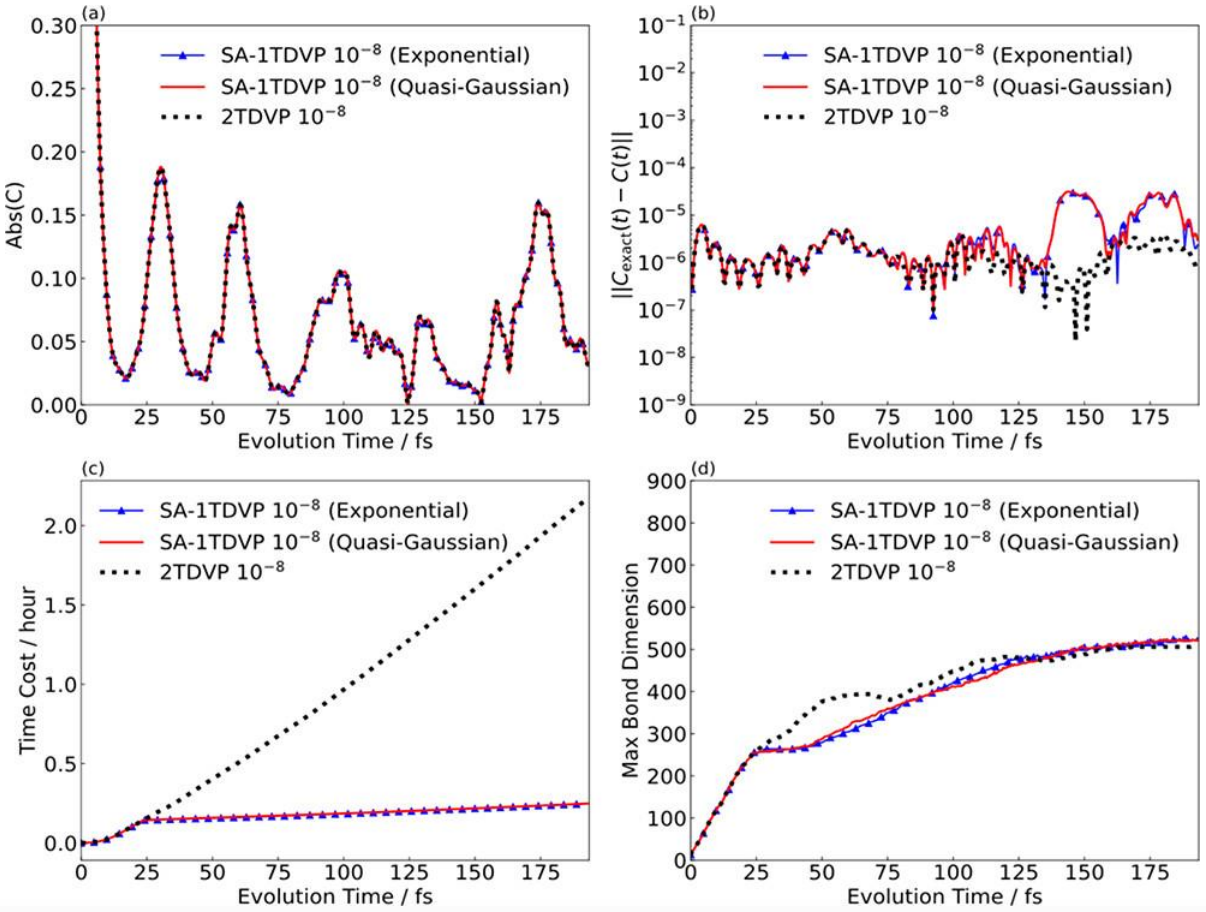

Two distributions for SA-1TDVP give similar performances and reduce ~80% computational time of 2TDVP.

Xu, Xie, Xie, Schollwöck, **Ma**, *JACS Au* **2022**, 2, 335.

SA-1TDVP

24-mode pyrazine

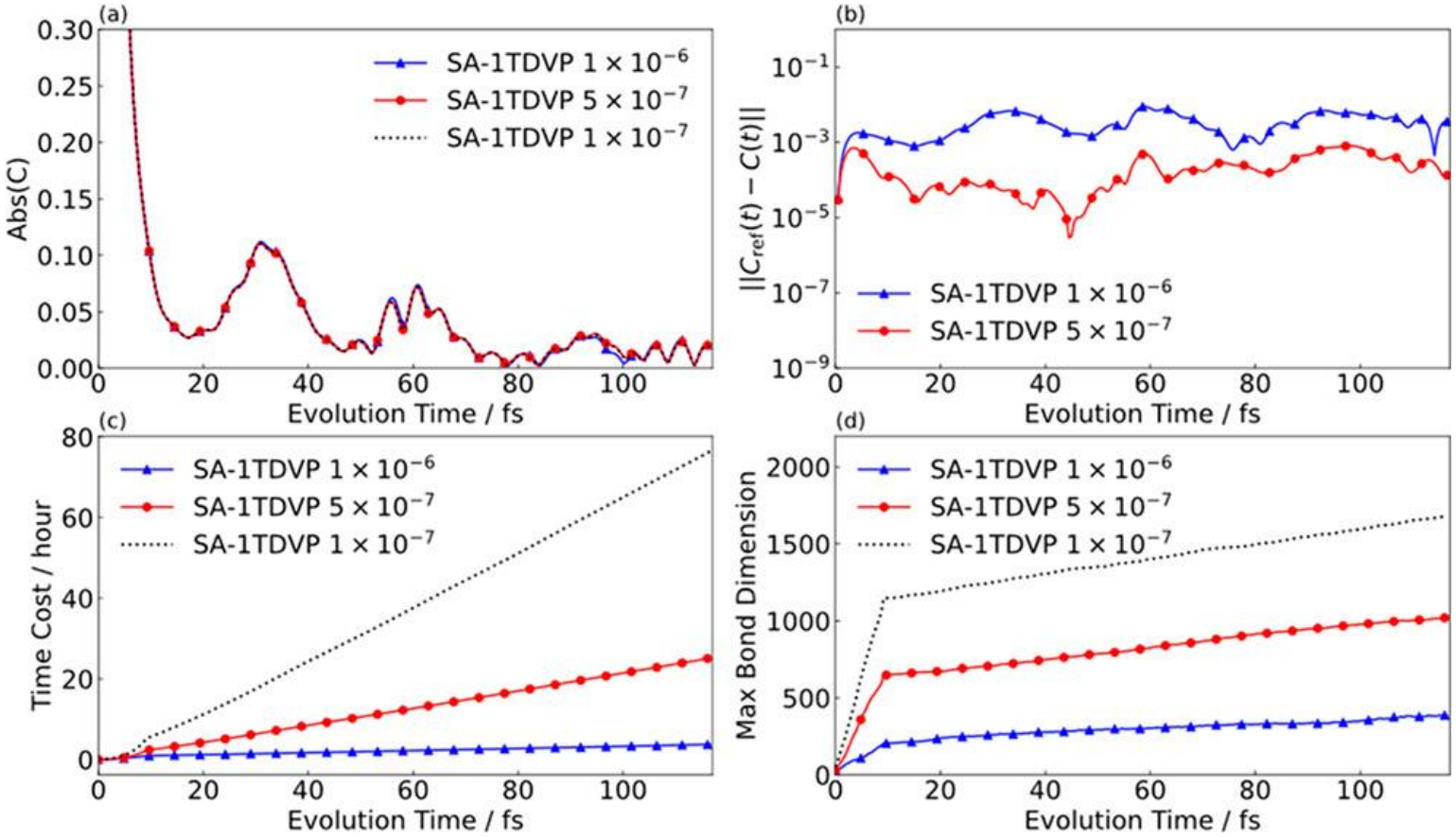

SA-1TDVP's error does not increase significantly as time evolves

SA-1TDVP

Simulated spectra of pyrazine and PBI

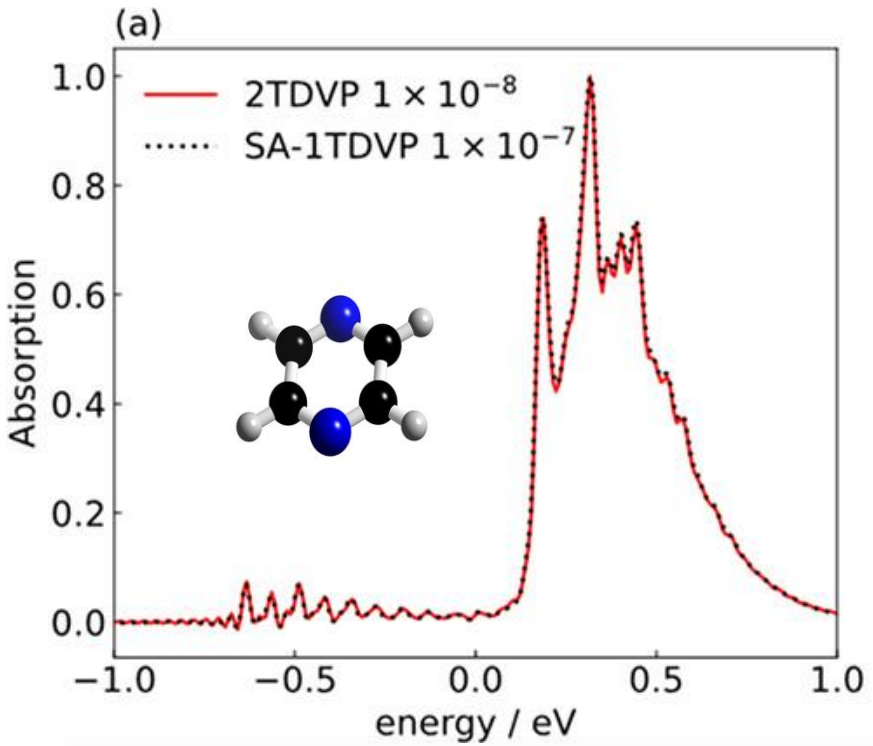

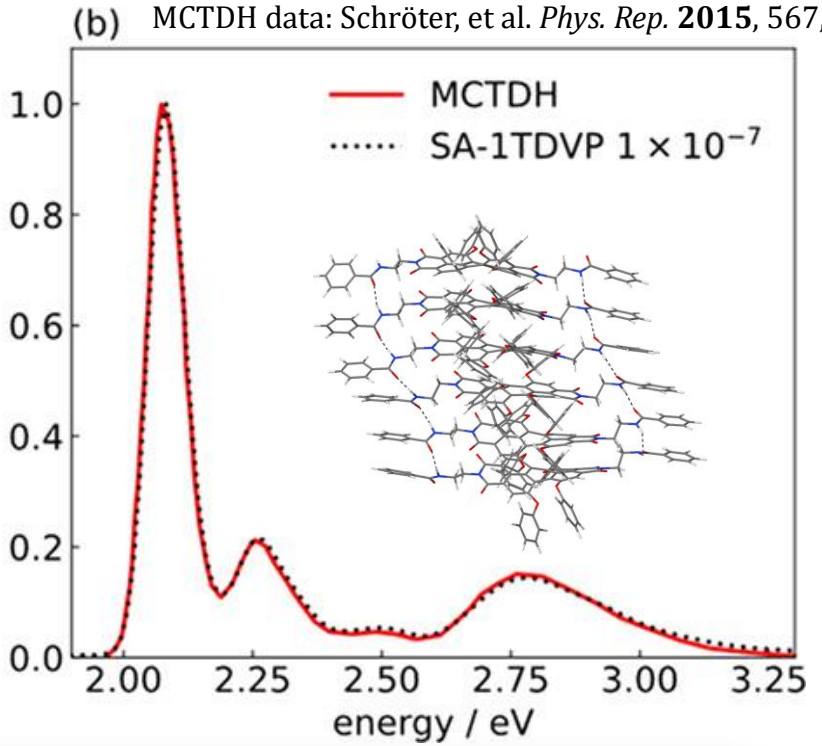

MCTDH data: Schröter, et al. *Phys. Rep.* **2015**, 567, 1.

SA-1TDVP can serve as an efficient and automatic tool for quantum dynamic and spectroscopy simulations.

Xu, Xie, Xie, Schollwöck, **Ma**, *JACS Au* **2022**, 2, 335.

SA-1TDVP

Application: exciton diffusion in 2D molecular crystal of PTCDI

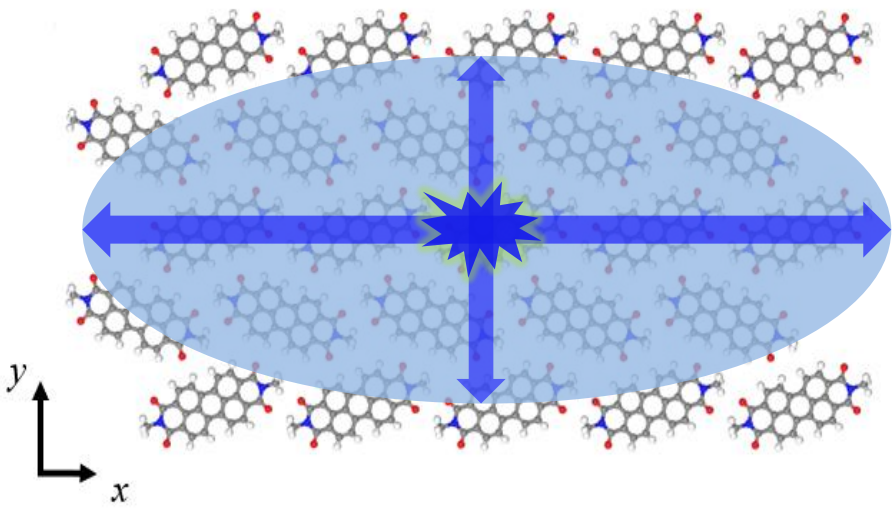

Zhao, **Ma**, Javey, Wang, et al., *Nat. Commun.* **2019**, 10, 5589.

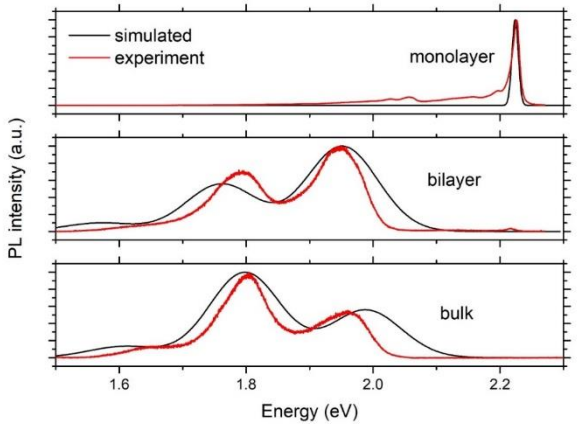

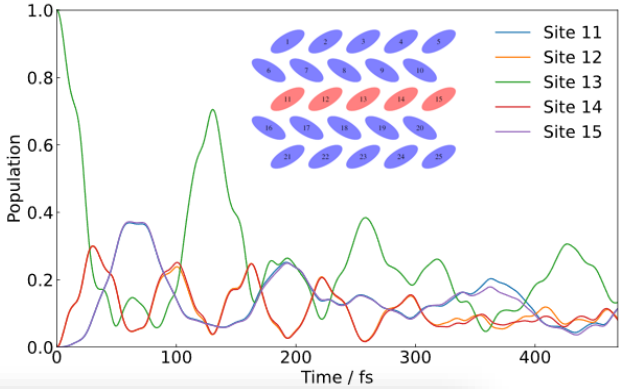

Strong anisotropy and J-aggregation effect

Xu, Xie, Xie, Schollwöck, **Ma**, *JACS Au* **2022**, 2, 335.

Summary

- BIPS provides an automatic and efficient scheme for the **accurate construction of the bases for excitonic models**. → **Model construction**
- **Ex-ph couplings** can be quantitatively evaluated by utilizing the locality of the electronic structures. → **Parameter evaluation**
- SA-1TDVP can **capture the entanglement growth adaptively and efficiently** in long-time simulations. → **Quantum dynamics**

Acknowledgement

Group members in NJU：




Ke Wang, Zhaoxuan Xie, Yihe Xu, Xiaoyu Xie

International collaborators：


Prof. Ulrich Schollwöck (LMU Munich)

Prof. Alessandro Troisi (Univ. Liverpool)

Thanks for your kind attention!